ENERGY RECOVERY IN THE REVERSE OSMOSIS PROCESS

Robert John Armstrong

ENERGY RECOVERY IN THE REVERSE OSMOSIS PROCESS

by

ROBERT JOHN ARMSTRONG

B.S., U.S. Naval Academy
(1967)

SUBMITTED IN PARTIAL FULFILLMENT

OF THE REQUIREMENTS FOR THE

DEGREES OF OCEAN ENGINEER

AND MASTER OF SCIENCE

at the

MASSACHUSETTS INSTITUTE OF

TECHNOLOGY

May, 1974

ENERGY RECOVERY IN THE REVERSE OSMOSIS PROCESS

by

ROBERT JOHN ARMSTRONG

Submitted to the Department of Ocean Engineering on May 9, 1974, in the partial fulfillment of the requirements for the degrees of Ocean Engineer and Master of Science in Naval Architecture and Marine Engineering.

ABSTRACT

The problem of finding an energy recovery turbine and a bootstrap pump for a reverse osmosis fresh water production system is examined. The primary objective is the minimization of the external power input required to produce a given amount of fresh water per day.

The examination of feasible reverse osmosis membrane performance parameters indicates that the optimal system nominal pressure is the lowest pressure which meets the applicable salt rejection criterion. For the system nominal pressure chosen, a ninety-degree radial-inflow hydraulic turbine is examined, and preliminary turbine design calculations are provided; a bootstrap pump on a common shaft with the turbine is selected, and a preliminary bootstrap pump design is provided; and a low pressure pump, required to produce the remaining system head, is selected, and a preliminary pump design is accomplished.

Thesis Supervisor: A. Douglas Carmichael
Title: Professor of Power Engineering

ACKNOWLEDGEMENTS

Professor A. Douglas Carmichael provided the impetus for this study; throughout the research and design phases of the thesis, he was ready with guidance and patience; his open door and subtle humor are greatly appreciated.

Pat and Squeaky kindly tolerated those inevitable times when "great" ideas and solutions became horrendous infeasibilities; for their patience and oft-needed encouragement throughout two theses and a design project, I am grateful.

TABLE OF CONTENTS

TABLE OF CONTENTS

LIST OF FIGURES

LIST OF TABLES

LIST OF SYMBOLS

Symbol	Description	Units
A	Area	ft^2
D	Diameter	ft
e_t	Efficiency, turbine overall	ft
h_{pk}	Stagnation pressure head at a point k	ft
Hn*	System nominal pressure head	ft
Hp*	Hydraulic head across pump	ft
Hp	Hydraulic head across a pump stage	ft
H_R*	Remaining hydraulic head	ft
H_t*	Hydraulic head across turbine	ft
H_t	Hydraulic head across a turbine stage	ft
H_{vapor}	Vapor pressure head	ft
K_u	Speed constant	
$\dot{m}$	Mass flow rate	lbm/sec
N	Rotative speed	rpm
n_t	Number of turbine stages	
n_p	Number of pump stages	
n_{lp}	Number of low pressure pump stages	
$N_{s,lp}$	Specific speed, low pressure pump	$rpm(gpm)^{1/2}/(ft)^{3/4}$
$N_{s,p}$	Specific speed, bootstrap pump	$rpm(gpm)^{1/2}/(ft)^{3/4}$
$N_{s,t}$	Specific speed, turbine	$rpm(cfs)^{1/2}/(ft)^{3/4}$
NPSH	Net positive suction head	ft
P_s	System nominal pressure	psia

LIST OF SYMBOLS

Symbol	Description	Units
P	Power	hp
Q	Volumetric flow rate	ft^3/sec
S	Suction specific speed	$rpm(gpm)^{1/2}/(ft)^{3/4}$
T	Torque	ft lbf
t	Blade height; vane height	ft
U	Peripheral velocity(blade speed)	ft/sec
V	Absolute velocity of fluid	ft/sec
W	Relative velocity of fluid	ft/sec
Z	Number of blades	
α	Angle	
β	Angle	
γ	Specific weight	$lbf/(ft)^3$
η	Efficiency	
ξ	Blade loading parameter	
ψ	Head coefficient	
ϕ	Capacity coefficient	
ω	Angular velocity	rad/sec
g	Local acceleartion due to gravity	$ft/(sec)^2$
g_c	Gravitational constant	lbm ft/lbf $(sec)^2$

SUBSCRIPTS

b	Brine
fw	Fresh water

SUBSCRIPTS

i	Inner (as in inner radius)
lp	Low pressure pump
o	Outer (as in outer radius)
p	Pump
r	Rotor tip
sw	Salt water
t	Turbine
m	Meridional
θ	Tangential

CHAPTER I
INTRODUCTION

Present steam-powered ships rely almost exclusively on the utilization of exhaust steam-operated distilling units to obtain fresh water. On most of those ships having propulsion plants other than steam, fresh water is obtained by one of the following three methods: 1) a supplemental ("donkey") boiler in combination with a low-pressure steam-operated distilling plant; 2) waste heat recovery distillation; and 3) vapor compression distillation. The exhaust steam-operated distilling plants are characterized by relatively short times between maintenance and/or repair. The supplemental boiler is both heavy and bulky. Not only is the waste heat recovery system heavy and bulky, but also its operation is a function of engine power settings. The vapor compression system is plagued by rapid scaling of the heat transfer surfaces, which requires frequent acid cleaning. Additionally, present ship design trends indicate increasing utilization of non-steam power plants with less space and weight allocated to propulsion and auxiliary (power and life support) systems. In view of the above, then, there is considerable interest in alternative processes for desalting sea water.

Reverse osmosis has emerged as a viable alternative process which can substantially reduce the weight, space, and power requirements for a shipboard fresh water-producing system. Additionally, it appears that reverse osmosis membrane technology is capable of producing membranes suitable for semi-annual replacement (for sea water plants); then the reverse osmosis system will possess a reliability which surpasses that of the current operational desalting systems.

In the reverse osmosis process, pressure in excess of the osmotic

pressure (approximately 25 atmospheres for sea water) is applied to obtain a fresh water yield through a selective semipermeable membrane. The semipermeable membrane is selected on the basis of its ability to reject the passage of dissolved salts. Since the sea water feed is pumped to a high pressure, and only a fraction of the feed water passes through the membrane as fresh water, there exists a brine effluent at a relatively high pressure. The brine effluent, then, possesses a potential for producing work through an energy-recovery device.

It is the objective of this thesis to accomplish a brief review of the reverse osmosis process, noting especially those parameters which impact on the potential for energy recovery; to design an energy recovery turbine to supply the input power to a high pressure "bootstrap" pump; to design the high pressure pump to be driven by the energy recovery turbine; and to design a low pressure pump to be driven by an external power source. A shipboard desalination plant application is stressed. Of primary importance is the minimization of external power required to yield one hundred thousand gallons per day of fresh water by reverse osmosis.

CHAPTER II
REVERSE OSMOSIS

II. A. General Description

Prior to examining the reverse osmosis process, the process of osmosis will be discussed. The history of osmosis can be traced back more than two centuries; e.g., in 1748 Abbe Nollet published the results of experiments on diffusion through animal membranes [15]. In order to have osmosis, there must exist a semipermeable membrane which is selective to the passage of certain components of a solution through the membrane. When two solutions of different concentrations are separated by a semipermeable membrane, there will be a tendency to equalize the two concentrations; this process usually results in the flow of solvent to the highly concentrated phase from the less concentrated solution. The flow of solvent from that solution rich in solvent to that solution less rich in solvent, i.e. to that solution which is more highly concentrated, is called osmosis.

It has been observed that the flow rate of solvent can be decreased if a pressure is applied to the highly concentrated solution. In fact, there exists a pressure at which, when applied to the highly concentrated solution, the flow of solvent will be reduced to zero. That pressure at which there is no solvent flow to the highly concentrated solution is an equilibrium pressure which is termed the osmotic pressure; the osmotic pressure is a pressure <u>difference</u> between the two solutions. Furthermore, if the pressure applied to the highly concentrated solution exceeds the osmotic pressure, there will be a reversal of the osmotic flow; i.e., solvent will pass from the highly concentrated solution to the less concentrated solution, and this process is termed reverse osmosis. For a more complete description of

the osmosis and reverse osmosis phenomena, see Reid [18], from which the above description was taken.

Since reverse osmosis depends on the use of a pressure in excess of the osmotic pressure, the reverse osmosis process has long been recognized as having potential application in the desalting of sea water to obtain fresh water. For example, the isentropic pump work required to pump water from atmospheric pressure to 1000 psia is approximately 3 BTU/lbm -- for a yield of 20 percent (i.e., 2 lbm fresh water per 10 lbm pumped and passed through the system), the isentropic pump work is then 15 BTU/lbm yield; alternately, the heat of vaporization of water at a typical flash distillation pressure is approximately 1000 BTU/lbm. With energy savings of an order of magnitude (or greater) possible, therefore, the reverse osmosis process has been the subject of increasing interest and research, primarily in the area of membrane technology. It is not the purpose of this thesis to review this research; rather, results of past and current research will be presented in terms of their impact on those parameters which affect the potential for energy recovery.

II. B. Determination of Important System Parameters

The characteristics of the reverse osmosis membrane separator unit itself largely determine the engineering design of the entire reverse osmosis plant. Therefore, a brief review of the performance characteristics of reverse osmosis membranes is important.

The performance of reverse osmosis membranes can be varied over wide ranges of salt rejection rates and fresh water recovery rates. Those variables which affect membrane performance can be conveniently separated into two groups: 1) membrane preparation and fabrication; and 2) operating conditions. The first area, i.e., membrane preparation and fabrication variables, is the subject of intense research; the interested reader is referred to the large number of Office of Saline Water (Department of the Interior) reports published annually. Since the objective of this thesis is to design an energy recovery system, which depends on membrane operating conditions, the following variables external to the membrane will be considered: system nominal pressure; system operating temperature; and Reynolds number (which relates flow and configuration variables).

Figure (1) shows the influence of the nominal driving pressure (defined as the system operating pressure minus the feed brine osmotic pressure) on the performance of a typical high-flux cellulose acetate membrane [14]. Figure (2) shows the influence of operating temperature on the performance of the same typical seawater desalination membrane [14]. And figure (3) shows the influence of Reynolds number on the performance of the same membrane. The following observations by Loeb are pertinent [14]:

a) The desalinized-water flux increases with increasing nominal driving

pressure, operating temperature, and Reynolds number; in the flow region studied, however, the Reynolds number variation was far less important than the other two parameters; and

b) The salt-reduction factor increases with increasing nominal driving pressure and Reynolds number; the salt-reduction factor is not a detectable function of the operating temperature.

It would appear, then, that in order to maximize the fresh water recovery rate ($\dot{m}_{fw}/\dot{m}_{sw}$), the system operating pressure should be increased to as high a level as possible. There are several further aspects which must be considered, however.

As the fresh water solvent is removed (by passage through the membrane), the concentration of the remaining brine increases. The osmotic pressure required to produce the fresh water flux is in fact a function of the salt concentration at the membrane surface, so that the required osmotic pressure may exceed that of the bulk solution [6], therefore requiring a greater pumping power. Furthermore, the salinity of the "fresh" product water increases as the salt concentration at the membrane surface increases. Additionally, Brian has observed that most saline water contains at least one salt at a concentration level not far below its solubility limit [6]; therefore an excessive concentration gradient may cause that salt to precipitate out at the membrane surface. And, membrane deterioration is hastened by both increasing operating pressure and increasing salt concentration at the membrane surface. Therefore, it is practicable to discard the brine while it retains much of its original fresh water solvent; hence, an upper limit to the desired fresh water recovery rate and the system operating pressure is necessary. The Office of Saline Water was contacted [13], and it was indicated that present research should conceivably yield

a membrane capable of producing at a fresh water recovery rate of 30 percent at 1500 psia, with a membrane life of six months.

It was noted above that the salt-rejection increases with increasing nominal driving pressure and Reynolds number. Since the minimum acceptable salt-rejection for a shipboard unit is about 99 percent, the operating pressure must be above a certain lower limit. During contact mentioned above with the Office of Saline Water, it was indicated that present research should conceivably yield a membrane capable of producing water at a sufficient quality of salt-rejection, at a pressure of 1000 psia; it was estimated that the fresh water recovery rate at this pressure would be 25 percent, at a bulk flow velocity of one to three feet per second.

The above arguments have determined upper and lower system pressure bounds. From figure (1), it can be seen that the desalinized-water flux is a linear function of pressure. Therefore, the upper and lower pressure bounds, with their accompanying water recovery rates, can be connected by a straight line as shown in figure (4). The equation representing this relationship is

$$\frac{\dot{m}_{fw}}{\dot{m}_{sw}} = 0.25 + \frac{0.05}{500}\,[P_s - 1000] \qquad (2.1)$$

where P_s=system nominal pressure, $1000 \leq P_s \leq 1500$ psia.

II. C. Basic Reverse Osmosis Plant Flow Diagram

A typical reverse osmosis plant will be described, and then a simplified process flow diagram will be presented. Salt water feed is collected in a tank; the water is treated with acids and chlorine in order to have proper chemical properties for passing through a membrane array. The water is passed through filters and a deaerator unit; it is then pumped to the system nominal pressure. As the salt water feed passes through the membrane separator unit, the high pressure forces the fresh product water through the membrane; the residual water (i.e., that water which did not pass <u>through</u> the membrane) has a somewhat higher salt concentration and is at a slightly lower pressure than the water entering the membrane separator unit. Since the brine effluent is still at a relatively high pressure, it possesses a potential for accomplishing work when passed through a hydraulic turbine. The fresh water product passes out of the array at nearly atmospheric pressure and is collected in a tank; the brine effluent is discharged overboard.

The above system is presented in a simplified schematic form in figure (5). Additionally, one important modification is made: the pumping unit has been split into two parts, one of which is driven by the energy recovery turbine in a "bootstrap" arrangement, and the other which is driven by an external power source.

Two important fundamental laws can be applied to the system shown in figure (5). The first, relating conservation of mass, yields the following set of equations (note that the numerical subscripts employed in this section refer to the points ① through ⑥ in figure (5), and do not follow

the subscript notation introduced in the List of Symbols):

$$\begin{aligned} \dot{m}_1 &= \dot{m}_2 = \dot{m}_3 = \dot{m}_{sw} \\ \dot{m}_4 &= \dot{m}_5 = \dot{m}_b \\ \dot{m}_6 &= \dot{m}_{fw} \\ \dot{m}_{sw} &= \dot{m}_{fw} + \dot{m}_b \end{aligned} \qquad (2.2)$$

The second fundamental law is the First Law of Thermodynamics, the application of which yields the following set of equations:

$$\begin{aligned} -\dot{m}_{sw}h_{p1} + \dot{m}_{sw}h_{p2} &= P_A \\ -\dot{m}_{sw}h_{p2} + \dot{m}_{sw}h_{p3} &= P_B \\ \dot{m}_b h_{p4} - \dot{m}_b h_{p5} &= P_D \end{aligned} \qquad (2.3)$$

where

P_A is the output power of pump A

P_B is the output power of pump B

P_D is the power removed from the fluid in passing though turbine D

h_{pk} is the stagnation pressure head at point k

when changes in elevation are neglected, and it is assumed that there is no head loss from pump A outlet to pump B inlet. An assumption commonly made (see, e.g., Bray in [5]) to account for pressure losses in a reverse osmosis plant, is that the summation of pressure losses occurs across the membrane separator unit and is 10 per cent of the system nominal pressure; then

$$h_{p4} = h_{p3} - 0.10h_{p3} \qquad (2.4)$$

If it is assumed that shaft losses from turbine D to pump B are negligible, then application of the concept of efficiencies yields an important result. The power output of pump B, when divided by its pump efficiency, yields the

power available for transmission to pump B. Then

$$P_D \eta_D = P_B/\eta_B \qquad (2.5)$$

Rearrangement of equation (2.5) yields the following equation:

$$P_D = \frac{P_B}{\eta_B \eta_B} \qquad (2.6)$$

A quick check of this equation confirms that as the product of the efficiencies of pump B and turbine D decreases, more power must be removed from the fluid passing through the turbine in order to yield the same power output of the pump.

In the previous paragraph, the continuity equation and the First Law of Thermodynamics were utilized to describe the system. An alternate approach would have been to utilize the Bernoulli equation in place of the First Law of Thermodynamics. In fact, the Bernoulli equation can be derived from a steady-flow form of the latter (the steady-flow energy equation), with assumptions of reversible and incompressible flow, and the presence of no shaft work. The flow under consideration is effectively incompressible, but the shaft work input is a major factor in the system, along with the inherent irreversibilities involved. The Bernoulli equation can be modified by inclusion of a head loss term, for irreversible flow; evaluation of the head loss term is not an explicit objective of this work; therefore, since the head loss is implicitly included in the First Law of Thermodynamics, the Bernoulli equation was not utilized. Further discussion of this point can be found in Daugherty and Franzini [8], Shepherd [19], and other texts on fluid mechanics.

In this chapter, the reverse osmosis process has been briefly reviewed; the parameters of membrane unit operation which affect the hydraulic turbine

and pump design have been determined; and a simplified system process diagram has been developed. In the next chapter, the process of selecting the appropriate machinery will be presented. And then the individual pump and turbine designs will be accomplished.

CHAPTER III
SELECTION OF PUMPING AND ENERGY RECOVERY EQUIPMENT

III. A. Introduction

In the previous two chapters the process of reverse osmosis has been briefly surveyed; the results of this survey were presented as figure (4), relating a range of fresh water recovery rates as a function over a domain of nominal system pressures. In fact, this functional relationship is sufficient in determining the important system parameters which will impact on the selection of appropriate pumping and energy recovery equipment.

It is readily apparent that, at the lower bound of the pressure domain, 1000 psia, less head must be input to a unit mass of feed water than at the upper bound of the pressure domain. However, since the fresh water recovery rate is lower at the lower bound of the pressure domain, a larger amount of feed water must be pumped up to 1000 psia. At the other extreme of the pressure domain, 1500 psia, the fresh water recovery rate is higher; although the input head per unit mass is greater, fewer units of mass must be pumped through the system in order to obtain the same yield of fresh water. In order to determine the system operating point which minimizes the amount of external energy required, it is necessary to select the equipment which will be utilized in the reverse osmosis plant shown in figure (5). Once the equipment components are selected, their particular operating characteristics (e.g., efficiency) can be utilized to converge toward a solution to the problem.

III. B. Specific Speed

Before embarking on a discussion of the various types of pumps and turbines available, it is useful to introduce a parameter which is commonly used by pump and turbine designers. This parameter is termed specific speed. When a dimensional analysis is applied to obtain relationships between the operating characteristics of pumps and turbines, and the properties of the fluid being utilized, the following two dimensionless groups have been shown (see Shepherd [19]) to be useful and are widely used:

$$\pi_1 = \frac{NQ^{1/2}}{H^{3/4}} \qquad \pi_2 = \frac{NP^{1/2}}{H^{5/4}}$$

where N is revolutions per time
Q is volume flow rate
P is power
H is hydraulic head

The first form of specific speed, π_1, is generally used for pumps since the effective performance quantities for pumps are head and flow rate; in this thesis, specific speed π_1 will be denoted by $N_{s,p}$. The second form of specific speed, π_2, is more commonly used for turbines, since the effective performance quantities for turbines are usually power and head; in this thesis, specific speed π_2 will be denoted by $N_{s,t}$.

In practice, the specific speed of a machine is evaluated at a point of maximum efficiency. Each different type of pump and turbine has its maximum efficiency within a relatively narrow range of specific speed. Therefore, when the operating requirements of a machine are determined, the specific speed is a significant parameter in determining which type of machine should be most suitable for a given application.

When the specific speed for a pump is determined, the speed N is usually expressed in revolutions per minute, flow rate Q in gallons per minute, and head H in feet. The resulting combination of units does not yield a dimensionless parameter; this combination is generally used. Therefore, in this thesis, whenever the specific speed of a pump is given, it will be in terms of Q gallons per minute, N revolutions per minute, and H feet. For evaluating the specific speed of a turbine, the units which will be used in this thesis correspond to common usage in the United States: N revolutions per minute, P horsepower, and H feet.

III. C. Preliminary Selection of Pumping Equipment

Pumps are commonly divided into two general types, positive displacement pumps and turbopumps; within each general type, further partitioning into subsets is possible. Positive displacement pumps change the pressure of a fluid by means of a sealed containment space with one or more moving boundaries. Turbopumps are characterized by both the fluid and the rotor having a significant dynamic motion: in a centrifugal pump, kinetic energy is imparted to the fluid being thrown outward to the casing; common examples of an axial pump are fans and propellers. The general domains of pump operation (in terms of head and capacity) where each is most efficient is presented in figure (6); taken from [11].

Hickman, et. al., have evaluated the various types of pumps available in terms of the operating requirements peculiar to a reverse osmosis desalinization plant [11]. After extensive evaluation, all positive displacement pumps other than reciprocating were rejected: those eliminated included gear pumps (water non-lubricating; pulsating output undesirable for the reverse osmosis membranes), lobe pumps (which fail to meet pressure and flow requirements), vane pumps (continuous high pressure would cause failure), screw pumps (which are heavy and bulky, and are not standard for the conditions required), flexible impeller pumps (cannot meet the high pressure requirements) and other less common types. And, since ship silencing is becoming even more important in the selection of shipboard equipment, the reciprocating pump is rejected. The remaining candidate pumps are turbopumps.

Turbopumps can be classified on the basis of the change in the radius

of the fluid flow through the pump. In a centrifugal pump, the liquid enters near the pump axis and is discharged at a much greater radius. In an axial flow pump, the flow does not undergo a significant change of radius. And between these two extremes, there are mixed-flow pumps. Schematic sketches of the types of rotating elements characteristic of each type of turbopump are shown in the bottom of figure (7).

Noting the geometry of the rotating elements in figure (7), the great significance of specific speed becomes readily apparent. The radial machine has a small inlet diameter; in order to avoid excessive entry velocities (which degrade efficiency), the flow rate must be restricted since the flow rate is proportional to the product of flow area and velocity. It can be shown that the head developed is proportional to the square of the product of rotative speed and external diameter. A low flow rate and a large developed head yield a low specific speed, since $N_{s,p}$ is proportional to $Q^{1/2}/H^{3/4}$, for radial pumps. At the other end of the spectrum, i.e. the axial pump, the flow area is not significantly limited -- therefore, a high flow rate is possible without having excessive entry velocities; since a row of blades can transfer but a limited amount of energy to the liquid under conditions of efficient operation, the specific speed for an axial pump will relate a high Q and a low H, and therefore result in a high value of $N_{s,p}$.

At this point in the analysis of candidate pumping equipment, the remaining feasible candidates are turbopumps: centrifugal, mixed-flow, and axial pumps. In order to obtain a compact unit, and to reduce the impact of axial thrust problems of either type of pump, it is desirable to couple the "bootstrap" pump and the hydraulic turbine on a common shaft.

Two of the characteristics which determine the pump specific speed, H and Q, have already been discussed. The remaining parameter, the rotative speed of the pump, N, must be determined; since a design objective is to have the pump and turbine joined by a common shaft (removing the requirement for a costly reduction gear, and yielding a lighter and smaller unit), the characteristics of the hydraulic turbine must be examined before the common shaft speed can be determined.

III. D. Preliminary Selection of Energy Recovery Equipment

As indicated in the earlier chapters, the brine discharged from the reverse osmosis array is at a high pressure, thereby possessing a potential for energy recovery. Energy recovery can be accomplished by passing the brine through a hydraulic turbine, or through a centrifugal pump operated as a turbine (i.e., centripetal rather than centrifugal flow). Hydraulic turbines can be designed to be quite efficient; a plot of hydraulic turbine efficiencies and specific speed ranges is presented in figure (8). When the fresh water recovery rates indicated in figure (4) are utilized (i.e., $0.25 \leq \frac{\dot{m}_{fw}}{\dot{m}_{sw}} \leq 0.30$) for a 100,000 gallon per day fresh water yield, feed water flow rates between 230 and 280 gallons per minute are feasible; when these flow rates are utilized as an input to figure (7), centrifugal pump efficiency is seen to be appreciably lower than the hydraulic turbine efficiencies indicated in figure (8); and, since Hickman, et. al., have shown the efficiency of a centrifugal pump used as a turbine to be lower than that of the pump [11], a centrifugal pump used as a turbine is rejected as a candidate energy recovery device.

The Pelton wheel is an impulse machine; the water flow is directed by jets to impinge on cups mounted on a rotating disk. The Pelton wheel can efficiently handle a low flow rate at a high head; however, the range of efficiency is severely limited (which could impact on the reverse osmosis system starting transient operation), requiring design to quite near a single point. The Francis turbine is seen to have efficient operation over a very broad range of specific speeds; additionally, the runaway conditions of a Francis turbine are satisfactory for the system being

considered. The Kaplan propeller turbine can have a large flow area, but is effective for but low heads; since the pressure drop will be on the order of 900 psia to 1350 psia, and a compact machine is desired, the Kaplan turbine is rejected. Therefore, the remaining candidate energy recovery device is the Francis turbine.

III. E. Determination of Pumping and Energy Recovery Equipment

Brief summary descriptions of pumping and energy recovery equipment have been provided; the pumping equipment candidates remaining after the initial screening process are all turbopumps -- centrifugal, mixed-flow, or axial, within a specific speed range of 500 to 15000 (see figure (7); and the sole remaining energy recovery equipment candidate is the Francis turbine, within a specific speed range of 15 to 100.

Figure (7) is the commonly used Worthington chart relating pump efficiency versus specific speed and flow rate. When the range of feasible flow rate is superposed on this diagram, it may be noted that the efficiency of the pump readily increases, until a specific speed of approximately 3000 is reached. It may also be noted that lower flow rates -- as utilization of parallel pumps would imply -- result in marked reductions in efficiency. Therefore, a set of centrifugal pumps in series, or a multistage centrifugal pump, operating at a specific speed near 3000 (in order to obtain the best efficiency for these flow rates), is to be selected.

Jenkins [12] utilized a limiting head per stage value of 500 ft for a hydrokinetic propulsion drive study, wherein the fluid possessed satisfactory lubricating characteristics. For this study, with seawater as the working fluid, a limiting head per stage of 400 ft is chosen. The seawater flow rates have been established by the relationship shown in figure (4). The remaining parameter in the determination of specific speed is the rotative speed. It appears that proposed designs for submarine applications will result in 20,000 rpm centrifugal pumps. For this study, a limiting rotative speed value of 15,000 rpm is chosen.

When a specific speed value of 3000 for the pump is utilized, a specific speed value for the turbine in the region of 20 is obtained. Reference to figure (8) shows a relatively flat efficiency curve for Francis turbine specific speed above 20 to 80. Since a Francis turbine specific speed above 20 requires an excessive rotative speed, and the efficiency of the turbine readily degrades below a specific speed of 20, a value of $N_{s,t} = 20$ is chosen for preliminary calculations.

Since the primary purpose of this thesis is the reduction of the external work input required to produce a given amount of fresh water, the work input to pump A in figure (5) is to be minimized. This minimization is accomplished as follows: a) the turbine power output is calculated; b) the turbine output power multiplied by the bootstrap pump efficiency yields the power developed across the bootstrap pump; c) the bootstrap pump head subtracted from the system nominal head yields the remaining head which must be developed across intake pump A, which will be termed the remaining head H_R*; and d) the product of the remaining head, the flow rate of seawater and the specific weight of the seawater, divided by the intake pump efficiency, yields the intake pump work. The details of the process and the results of the calculation are presented in Appendix A.

The results of the process accomplished in Appendix A are presented in figure (9). Six pressures, 1000 psia through 1500 psia in 100 psia intervals, were utilized, and a smooth curve resulted. Since the curve in figure (9) is monotonic in nature, a refined program to evaluate the entire pressure domain from 1000 psia to 1500 psia is not necessary. From figure (9) it is readily apparent that the minimum external power requirement occurs at a system nominal pressure of 1000 psia. This result can

be stated in another way: that power generated by the passage of a decreased flow rate of brine through a greater pressure difference across the hydraulic turbine is insufficient, when evaluated in terms of energy reduction, to justify the additional power required to raise the feed water to a higher system nominal pressure.

In this chapter, the pumping and energy recovery equipment in the simplified reverse osmosis system of figure (5) has been evaluated in terms of minimizing the external energy required to yield a fixed amount of fresh water per day. It was determined that the objective was satisfied when the system nominal pressure was at its lower bound consistent with satisfactory membrane performance. This lower bound system nominal pressure, 1000 psia, will therefore set the important parameters required for a detailed pump and recovery turbine design, which is presented in the following chapter.

CHAPTER IV
Pump and Recovery Turbine Designs

IV. A. Basic Theory

In the previous chapter, an examination of external energy requirements led to selection of a reverse osmosis system with a nominal pressure of 1000 psia. In the present chapter, a detailed design of the three principal pieces of turbomachinery -- the energy recovery turbine, the bootstrap pump, and the low pressure pump -- will be discussed; the process and details of the calculations are presented in Appendix B, C, and Appendix D, respectively.

A basic law on which the field of turbomachinery is based, is the principle of conservation of angular momentum: the sum of the moments of external forces acting on a system is equal to the rate of change of the moment of momentum of the system, when both are referenced to the same point. Assuming steady flow, taking rotation about the axis of rotation of the turbomachine rather than about a point, and utilizing properties at a point which respresent a single mean value for the flow passing in the region of that point, Euler's equation for single stage pump or turbine torque can be readily derived:

$$T = \frac{\dot{m}}{g_c} (R_2 V_{\theta 2} - R_1 V_{\theta 1}) \qquad (4.1)$$

where T is torque
$\dot{m}$ is the mass flow rate of fluid
R_2 is the discharge radius
$V_{\theta 2}$ is the tangential component of the absolute discharge velocity
R_1 is the entrance radius
$V_{\theta 1}$ is the tangential component of the absolute entrance velocity

Several observations regarding equation (4.1) are in order: a) the torque

depends on the mass flow rate and on the tangential components of the absolute (actual) velocities -- the other component of absolute velocity, the radial component, passes through the origin and therefore has no effect on the torque; b) the equation relates the actual torque and therefore does not need to have an efficiency included; and c) the use of mean value properties is a convenience often utilized in initial design calculations for a representative point -- the torque over the whole turbomachine could be obtained by integrating for the entire flow (including boundary layers). Figure (11) shows the absolute velocity of flow leaving a rotating element (rotating at constant counterclockwise angular velocity ω), and the tangential and radial components of the absolute velocity. Equation (4.1) is readily applicable to pumps and turbines.

For a pump, with blades extending from the entrance, at inner radius R_i, to the discharge, at outer radius R_o, there can be no flow through the blade surfaces, so the fluid enters and leaves only about the circumference inscribed by R_i and R_o. If the entering and leaving velocities are both in the same direction as the direction of rotation, then $V_{\theta 1}$ and $V_{\theta 2}$ are positive quantities. Then equation (4.1) becomes

$$T = \frac{\dot{m}}{g_c} (R_o V_{\theta 2} - R_i V_{\theta 1}) \qquad (4.2)$$

and T is the external torque which must be applied to the rotor; this torque increases the angular momentum of the fluid and can be seen as an increase in pressure and kinetic energy. Torque is transmitted by the shaft at a rate of ω radians per second; the pump power is readily obtained:

$$P = T\,\omega = \frac{\dot{m}}{g_c}\,(R_o V_{\theta 2} - R_i V_{\theta 1})\,\omega$$

Since $\omega R = U$, the blade speed at a radius R,

$$P = \frac{\dot{m}}{g_c}\,(U_o V_{\theta 2} - U_i V_{\theta 1}) \tag{4.3}$$

For the turbine, with flow from the entrance, at outer radius R_o, to the discharge, at inner radius R_i, the flow is again only about the circumference inscribed by R_i and R_o. Then application of equation (4.1) yields

$$T = \frac{\dot{m}}{g_c}\,(R_i V_{\theta 2} - R_o V_{\theta 1}) \tag{4.4}$$

If $V_{\theta 2}$ is negative, i.e. directly opposed to the rotation (although, in general, it can be in either direction), then equation (4.4) can be written as

$$T = -\frac{\dot{m}}{g_c}\,(R_o V_{\theta 1} - R_i V_{\theta 2}) \tag{4.5}$$

In equation (4.5) the torque is a negative quantity, indicating that torque is not put into the fluid, but rather removed from it. Expressing equation (4.5) in terms of power

$$P = -\frac{\dot{m}}{g_c}\,(U_o V_{\theta 1} - U_i V_{\theta 2}) \tag{4.6}$$

where it is understood that P is a positive quantity representing the power out from the turbine.

From the foregoing development, it is readily apparent that the important factors in the production or utilization of power in a turbomachine are the mass flow rate, the absolute flow velocities, the tangential components of the absolute flow velocities, machine geometry, rotative speed, and blade speed. For the system under consideration

the feed water flow rate has been determined with the selection of the system nominal pressure; similarly, since a fresh water recovery rate of 0.25 lbm fresh water/1 lbm salt water feed has been determined at the selected pressure, the brine flow rate through the recovery turbine is established. The flow velocities and their components are determined by entrance and discharge velocity diagrams. The rotative speed has been determined in the previous chapter, in order to maintain an appropriate specific speed. The blade speed and rotative speed are related by machine geometry. Therefore, the remaining important variables to be examined in the detailed design are the following: a) machine geometry; b) absolute flow velocities; and c) the flow velocity diagrams. As indicated in Chapter III, the appropriate order of the design process is as follows: a) the energy recovery turbine; b) the bootstrap pump; and c) the low pressure pump.

IV. B. Detailed Recovery Turbine Design

From the examination in Chapter III, a Francis-type reaction turbine was chosen. The principal component in the Francis turbine which acts in the conversion of hydraulic energy to mechanical energy is the runner. The specific speed of the Francis turbine has been set at 20, in order to permit maximum bootstrap pump efficiency, as described in Chapter III. When this value of specific speed is utilized as an input (after conversion to the European non-dimensional form of specific speed) to the curves in Bovet ("Progressive change of form of runner passage as function of specific speed n") [4], the Francis runner is effectively a 90° radial inflow turbine rotor. Therefore, the procedure presented by Carmichael [7], which has been utilized by Jenkins [12] and Potter [17], for the design of 90° radial inflow turbines -- with simplification for incompressible flow -- will be followed in this thesis.

As described in the previous section, the brine flow rate through the turbine has been set as a parameter by the reverse osmosis array performance characteristics. Additionally, with the system nominal pressure set at 1000 psia, and with an assumed back pressure in the turbine of 25 psia, the total head across a turbine stage has been set. Therefore, the power output for a turbine stage is determined. Utilization of Euler's equation will lead to determination of the velocity triangles at rotor inlet and outlet, with the major assumption that the absolute velocity leaving the rotor has no swirl (tangential) component. If the gap between the stator outlet and the rotor inlet is small, and the moment of momentum remains constant across this gap, then the stator

outlet velocity triangle will be effectively the same as that of the rotor inlet. With an assumed value of the pitch (radial spacing between stator blades) - chord ratio, the stator inlet velocity triangle can be determined. Design of the scroll for the first turbine stage completes the process -- since the flow leaving the first and second stages is already distributed about the stator entrance for the following stages, simple flow passages are utilized. The details of the design process and the calculations for the system nominal pressure under consideration are presented in Appendix B.

IV. C. Detailed Bootstrap Pump Design

From the examination in Chapter III, a centrifugal pump was chosen. The principal component in the centrifugal pump which acts in the conversion of mechanical energy to hydraulic head is the impeller. The salt water feed enters the impeller in a central portion around the shaft, called the eye, and after flowing radially outward, is discharged into a casing which extends about the entire pump circumference. That energy which is imparted to the salt water by the vanes is manifested by an increase in both pressure and absolute velocity; the conversion of the kinetic energy to hydraulic head is accomplished in a diffuser of a volute. Since all of the head is generated by the impeller, the design of the impeller, in terms of velocity triangles and geometry, is the most important aspect of a centrifugal pump design. The other portions of the pump incur losses but do not generate head. Although current designs have produced pumps with high overall efficiencies, the design procedure is based almost entirely on utilization of "design factors" which have been established experimentally from successful earlier designs. The procedure presented by Stepanoff [21], wherein a number of ratios -- again it must be emphasized that these ratios are almost entirely experimental, not lending themselves to a rigorous theoretical treatment -- are utilized, will be followed in this thesis.

As described in the previous section, the salt water feed flow rate through the bootstrap pump has been set as a parameter by the reverse osmosis array performance characteristics. With the determination of the power produced by the recovery turbine, the total head developed

across a bootstrap stage can be determined in a manner described in Appendix A. Since the bootstrap pump is directly coupled to the recovery turbine, the rotative speed of the pump is determined. And, since the bootstrap pump specific speed is set by a combination of the rotative speed, head developed per stage, and salt water flow rate, the primary parameter for entering the curves presented in Stepanoff [21] is determined. The details of the bootstrap pump design process and the calculations for the system nominal pressure under consideration are presented in Appendix C.

increase in fluid velocity, or deviation of flow streamlines. Cavitation manifests itself by the presence of one or more of the following occurrences, all of which are detrimental to pump performance and pump life: a) noise and vibration; b) cavitation corrosion and fatigue in metal parts; and c) cavitation pitting.

There are several factors available to the pump designer who is attempting to produce a cavitation-free design. Percival [16] gives a satisfactory survey of three common cavitation correlations -- Prandtl's cavitation number, Thoma's cavitation constant, and the suction specific speed -- and detailed review of these herein is not necessary. An important term in two of the three common cavitation correlations is the net positive suction head (NPSH). The net positive suction head relates the total head above vapor head at the impeller entrance:

$$NPSH = H + \frac{V_{mi}^2}{2g} - Hvapor$$

A parameter which relates the net positive suction head to rotative speed and flow rate, in a manner analogous to the definition of specific speed, is the suction specific speed for pumps:

$$S = N\, Q^{1/2}\, (NPSH)^{-3/4}$$

Although Percival [16] cites specially designed pumps which operate at a suction specific speed of 34000, and Stepanoff [21] cites operation of specially designed pumps at suction specific speeds approaching 15000 (as of 1957), the Hydraulic Institute recommends a limiting suction specific speed below 8500. A limiting suction specific speed value of 8000 will be utilized in this thesis.

As described earlier in this chapter, setting of the system nominal pressure has determined the salt water feed flow rate through the pumps. Carmichael [7] has suggested that, in order to have the low pressure pump operate with characteristics similar to those of the bootstrap pump, the specific speed of the low pressure pump should be the same as that of the bootstrap pump; this assumption will be followed in this thesis. The details of the low pressure pump design process and the calculations for the system nominal pressure under consideration are presented in Appendix D; after some initial calculations which indicate the impact of cavitation on the pump design, as well as determination of the remaining head, the procedure suggested by Stepanoff, and presented in slightly modified form in Appendix C in this thesis, will be utilized.

CHAPTER V
CONCLUSIONS AND RECOMMENDATIONS

V. A. Conclusions

From this study of energy recovery and pumping systems for a reverse osmosis system, several conclusions may be made. First, if the primary parameter of interest is the total amount of external power input required, the lowest pressure feasible system is the optimal selection; the lowest pressure feasible system is that system which operates at a pressure sufficient to satisfy salt rejection criteria such that the quality of the fresh water product is high enough to meet the applicable potable water standards.

Second, the preliminary calculations herein suggest that a plant output of at least 100,000 gallons per day is required: the outer diameters of the pumps and turbine rotating elements for this size plant are in the range of three inches -- the blade heights are such that, if they be decreased, penalties in pump and turbine efficiency will result due to the small passage sizes. This fresh water yield, then, is applicable to only the larger commercial and military ships; additionally, such a plant would have ready application on islands or in areas with poor power distribution systems (e.g., a resort developer in lower Baja California has shown interest in this study). Further, with regard to the fresh water yield, another conclusion is possible: due to the nature of the pump efficiency curve, flow rates for systems with a larger yield will show an economy of scale, since the pump efficiency readily increases in the appropriate specific speed range with increased flow rates of salt water feed.

Third, if system life cycle cost is the primary parameter of interest, preliminary calculations indicate that the lowest pressure feasible system also has the lowest life cycle cost. Assumptions made to arrive at this conclusion are the following: a) membrane initial cost is $0.25 per square foot; b) membrane replacement is accomplished every six months, for a twenty year period; c) membrane replacement cost is $0.25 per square foot; d) power cost is $0.01 per KW-hr; and e) the discount rate is 10 percent.

V. B. Recommendations

The reverse osmosis energy recovery and pumping system has been approached from only the perspective of minimizing the amount of external power required to produce a given amount of fresh water per day. Other important considerations to the marine engineer are weight, volume, cost and reliability. Insufficient published data regarding pump and turbine weight and volume (in the applicable head and flow capacity regions) exists to permit a system optimization with regard to these two important variables.

Although the trend in reverse osmosis membrane research has been to find sea water membranes operating at higher pressures (and thereby yielding a higher amount of fresh water per pound of salt water feed), this study suggests that the research concentrate on the lower pressure membranes: improving the reliability and decreasing the costs of the lower pressure membranes will directly result in energy savings as well as cost reductions for the overall reverse osmosis system analyzed in this thesis.

[1] Addison, H., Centrifugal and Other Rotodynamic Pumps, London: Chapman & Hall, 1966.

[2] Balji, O.E., "A Study on Design Criteria and Matching of Turbomachines: Parts A and B", Journal of Engineering for Power, Transactions of the ASME; Vol. 84, Series A, No. 1, January 1962.

[3] Baumeister, Theodore, and Lionel S. Marks, Standard Handbook for Mechanical Engineers, New York: McGraw-Hill Book Co., 1967.

[4] Bovet, Theodore, "Contribution to the Study of Francis-Turbine Runner Design", ASME Publication 61-WA-155, New York, 1962.

[5] Bray, D.T., "Engineering of Reverse-Osmosis Plants", in Ulrich Merten, ed., Desalination by Reverse Osmosis, Cambridge, MA: The M.I.T. Press, 1966.

[6] Brian, P.L.T., "Mass Transport in Reverse Osmosis", in Ulrich Merten, ed., Desalination by Reverse Osmosis, Cambridge, MA: The M.I.T. Press, 1966.

[7] Carmichael, A. Douglas, Lectures in Subject 2.601 at M.I.T., 1973-1974, and personal conversations.

[8] Daugherty, Robert L. and Joseph B. Franzini, Fluid Mechanics with Engineering Applications, New York: McGraw-Hill Book Company, 1965.

[9] Friedlander, G.D., "Science and the Salty Sea", in Sumner N. Levine, ed., Desalination and Ocean Technology, New York: Dover Publications, 1968.

[10] Gollan, A., "Hydrocasting Reverse Osmosis Membranes, Development of Porous Support Tubes, Study of the Mechanism of Membrane Formation and Development of Non-Cellulosic Desalination", Hydronautics, Inc. Report, 1973.

[11] Hickman, K.E., et al., Pumping and Energy Recovery Systems for Reverse Osmosis Desalination Plants, Cambridge, MA: Dynatech R/D Company, 1969.

[12] Jenkins, Thomas H., "Hydrokinetic Propulsion Drives; A Feasibility Study", unpublished thesis, Department of Ocean Engineering, M.I.T., May 1973.

[13] Telecon with Dr. Lee Kindlay, Head of OSW Research Group, OSW, Department of the Interior, 1974.

[14] Loeb, S., "Preparation and Performance of High-Flux Cellulose Acetate Desalination Membranes", in Ulrich Merten, ed., Desalination by Reverse Osmosis, Cambridge, MA: The M.I.T. Press, 1966.

[15] Merton, Ulrich, "Reverse Osmosis" in Sumner N. Levine, ed., Desalination and Ocean Technology, New York: Dover Publications, 1968.

[16] Percival, Robert C., "Optimization of Waterjet Pumps for Hydrofoil Application", unpublished thesis, Department of Ocean Engineering, M.I.T., June 1972.

[17] Potter, David, "Preliminary Turbine Design for Thermal Cycle Feasibility", unpublished Master's thesis, Department of Ocean Engineering, M.I.T., May 1974.

[18] Reid, C.E., "Principles of Reverse Osmosis", in Ulrich Merten, ed., Desalination by Reverse Osmosis, Cambridge, MA: The M.I.T. Press, 1966.

[19] Shepherd, Dennis G., Elements of Fluid Mechanics, New York: Harcourt, Brace, & World, Inc., 1965.

[20] Smith, C.K., "Test and Evaluation of an 80,000 GPD Reverse Osmosis Seawater Desalination Plant Mounted on an Ammi Pontoon", Naval Civil Engineering Lab Report, 1974.

[21] Stepanoff, A.J., Centrifugal and Axial Flow Pumps, New York: John Wiley & Sons, Inc., 1957.

[22] "The Mechanism of Desalination by Reverse Osmosis", by Aerojet-General Corporation, OSW Research and Progress Report No. 34, 1963.

[23] "Waterjet Propulsion System Study, Report No. 2--Pump Selection and Design", Lockheed Contract NObs-88605, September 1965.

[24] "Waterjet Propulsion System Study, Report No. 5--System Design and Analysis", Lockheed Contract NObs-88605, September 1965.

[25] Wislicenus, G.F., Fluid Mechanics of Turbomachinery, New York: Dover Publications, 1965.

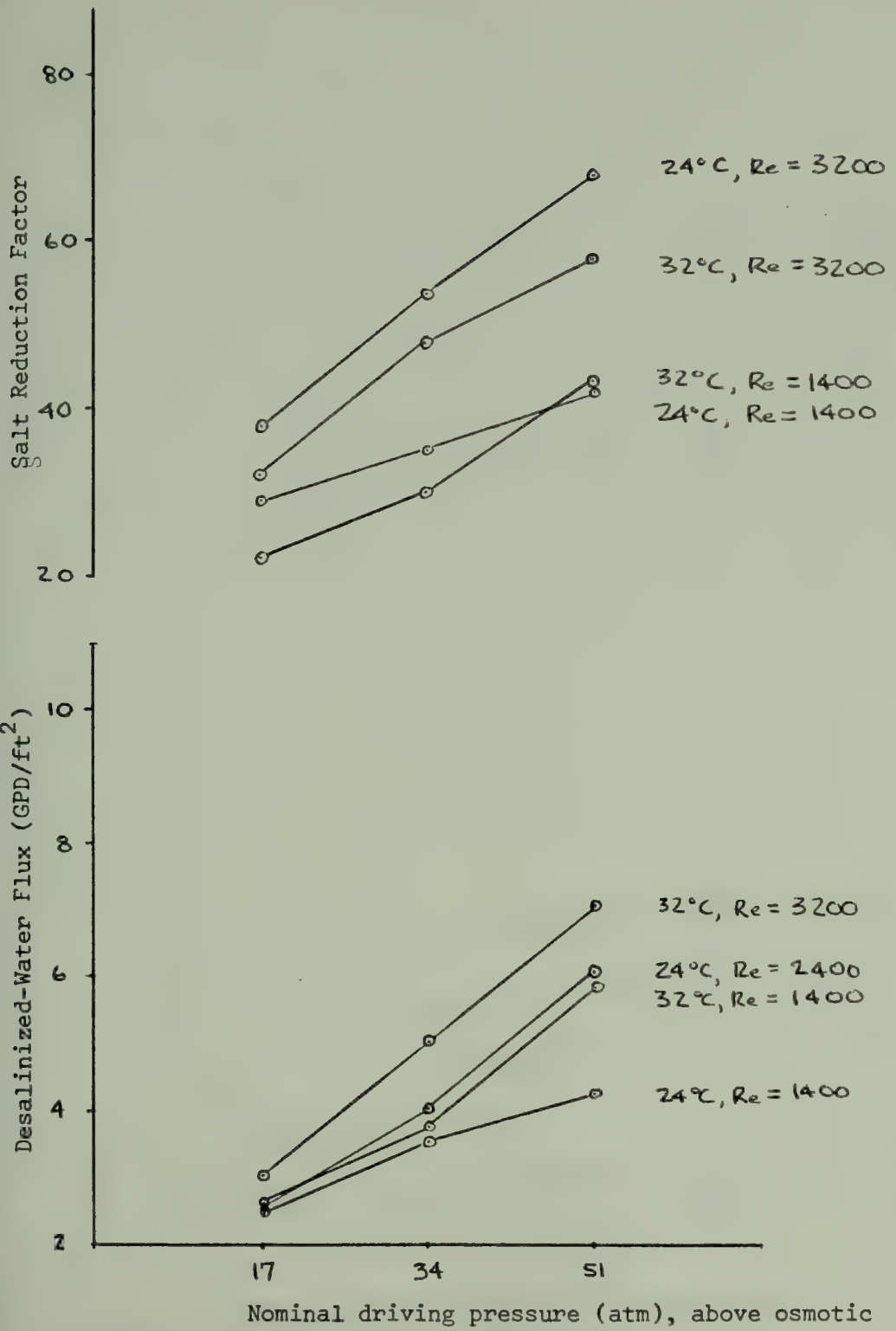

Figure (1): Influence of nominal driving pressure on seawater R/O membrane performance

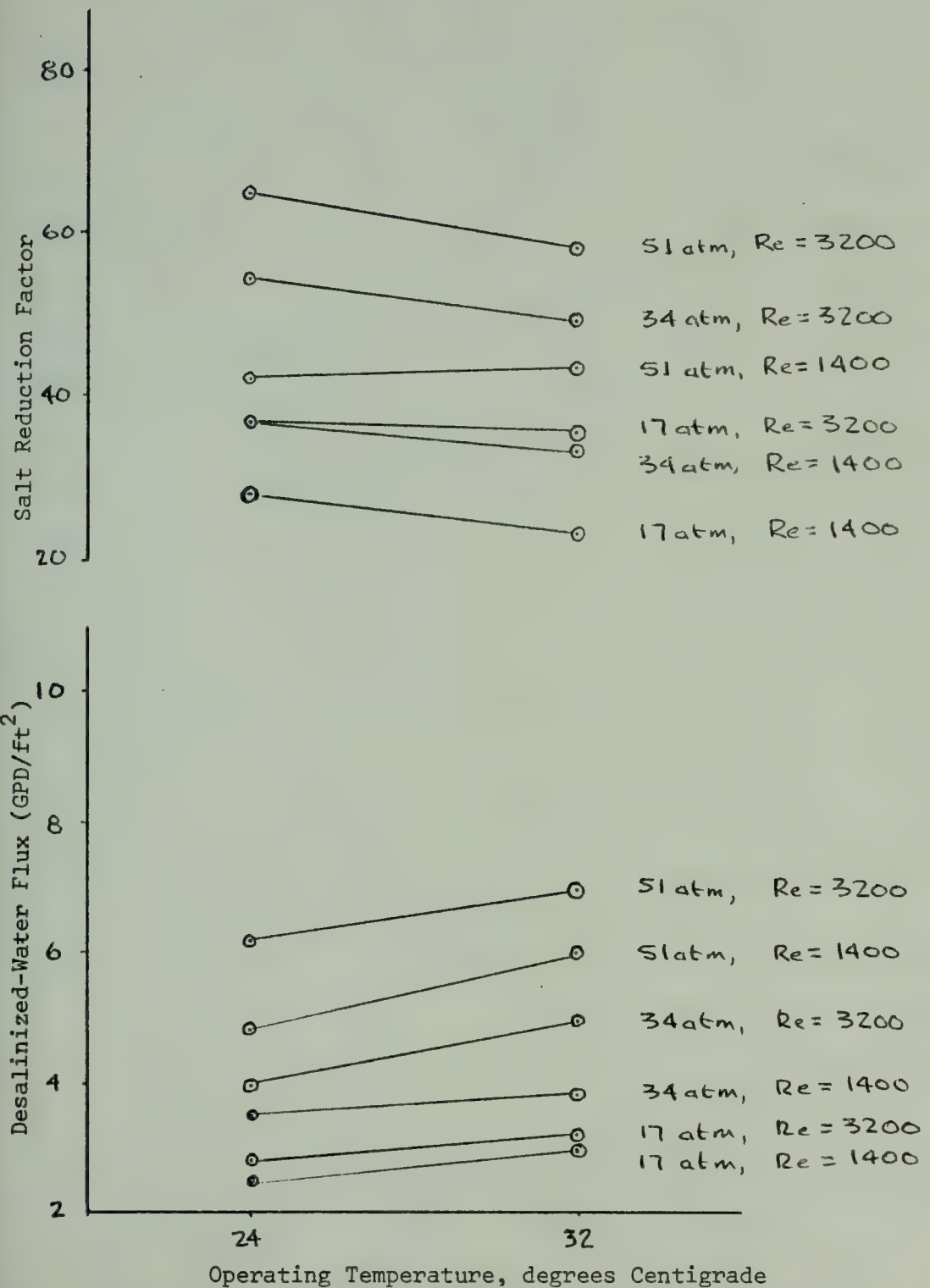

Figure (2): Influence of operating temperature on seawater R/O membrane performance

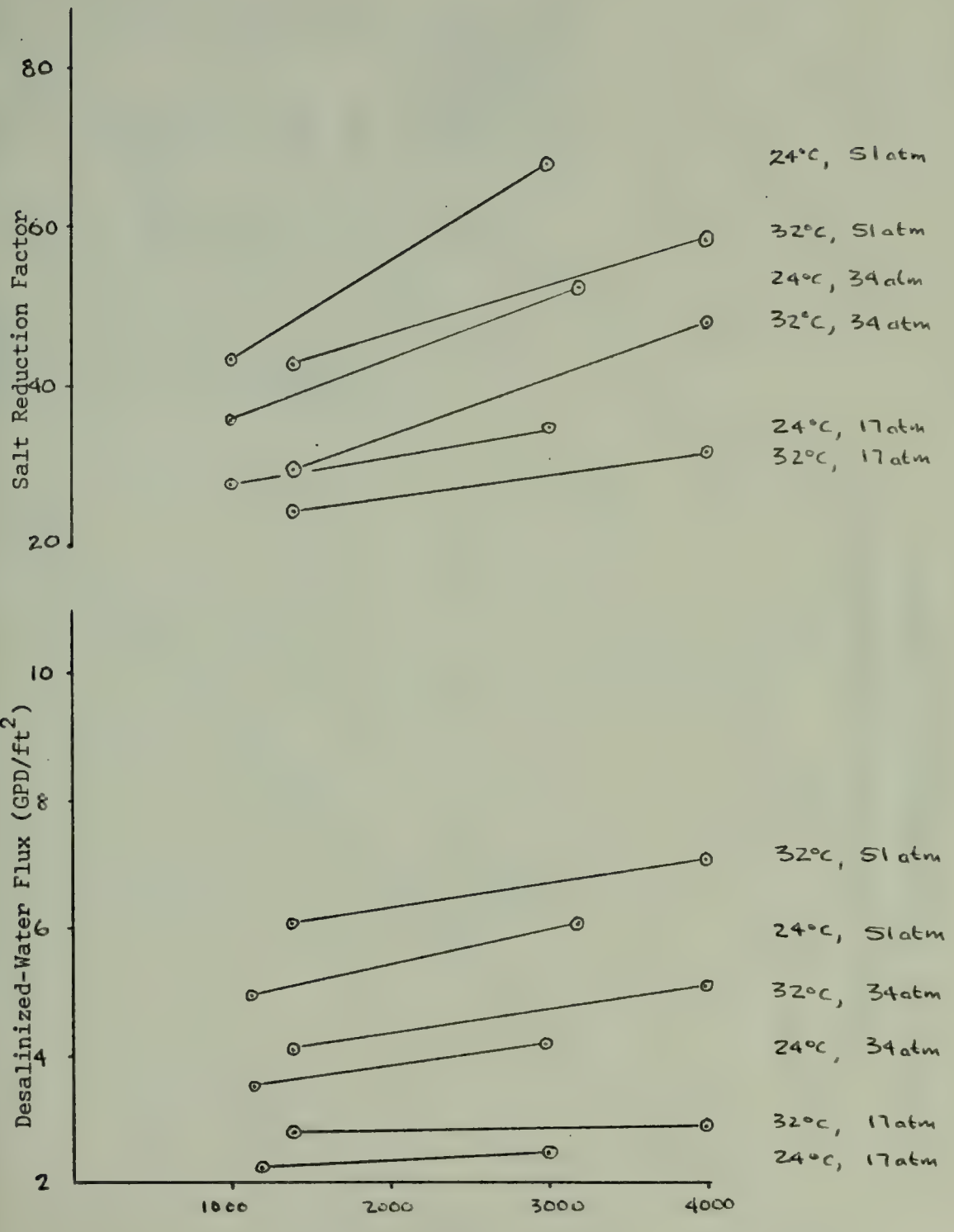

Figure (3): Influence of Reynolds number on seawater R/O membrane performance

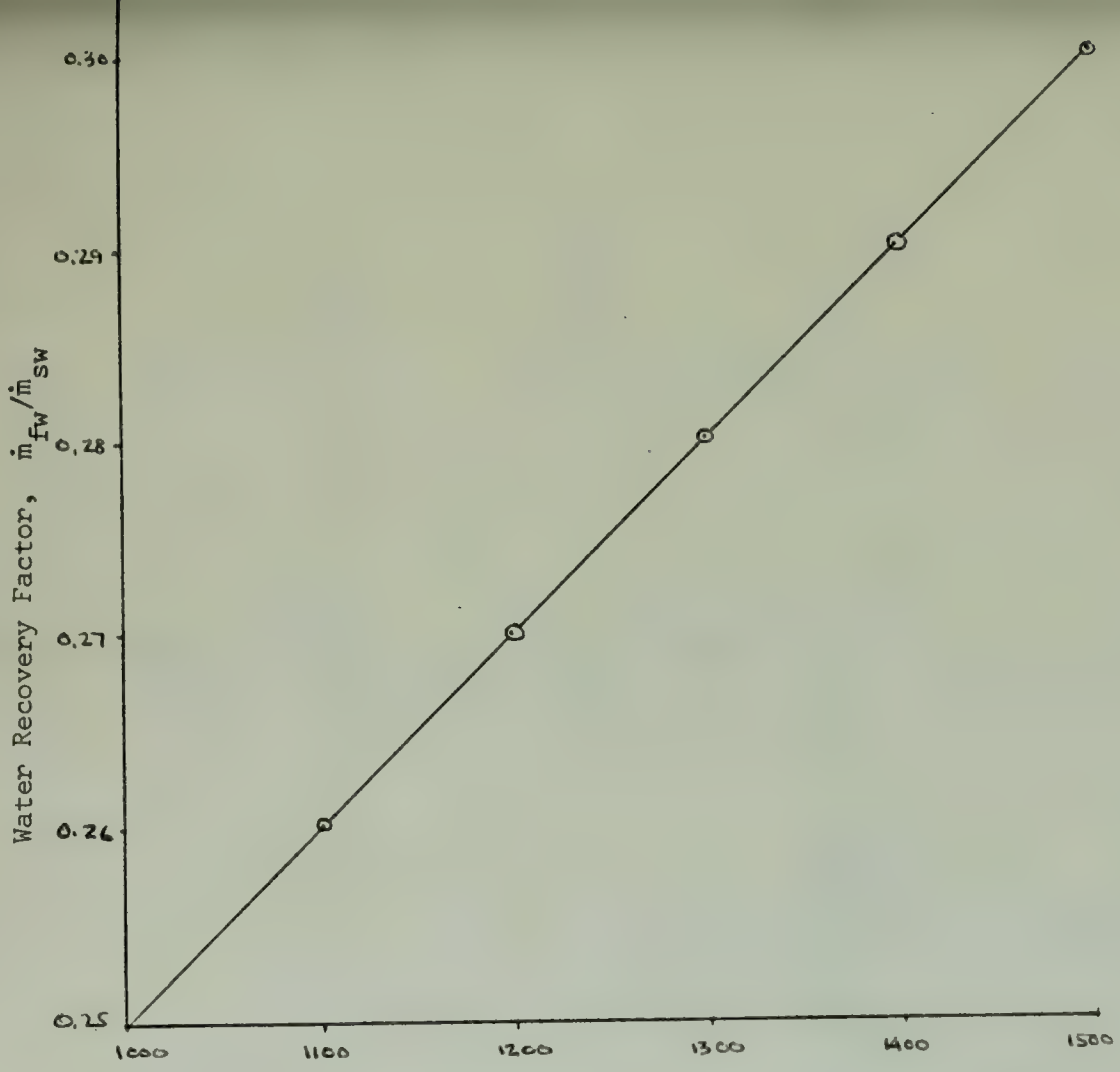

Figure (4): Water recovery as a function of system nominal pressure

Pressure	m_{sw}	m_b	m_{fw}
1000	277.8	208.3	69.4
1100	267.0	197.6	69.4
1200	257.2	187.7	69.4
1300	248.0	178.6	69.4
1400	239.6	170	69.4
1500	231.6	162	69.4
psia	gpm	gpm	gpm

Table 1: Brine, salt water, and fresh water flow rates as a function of system pressure

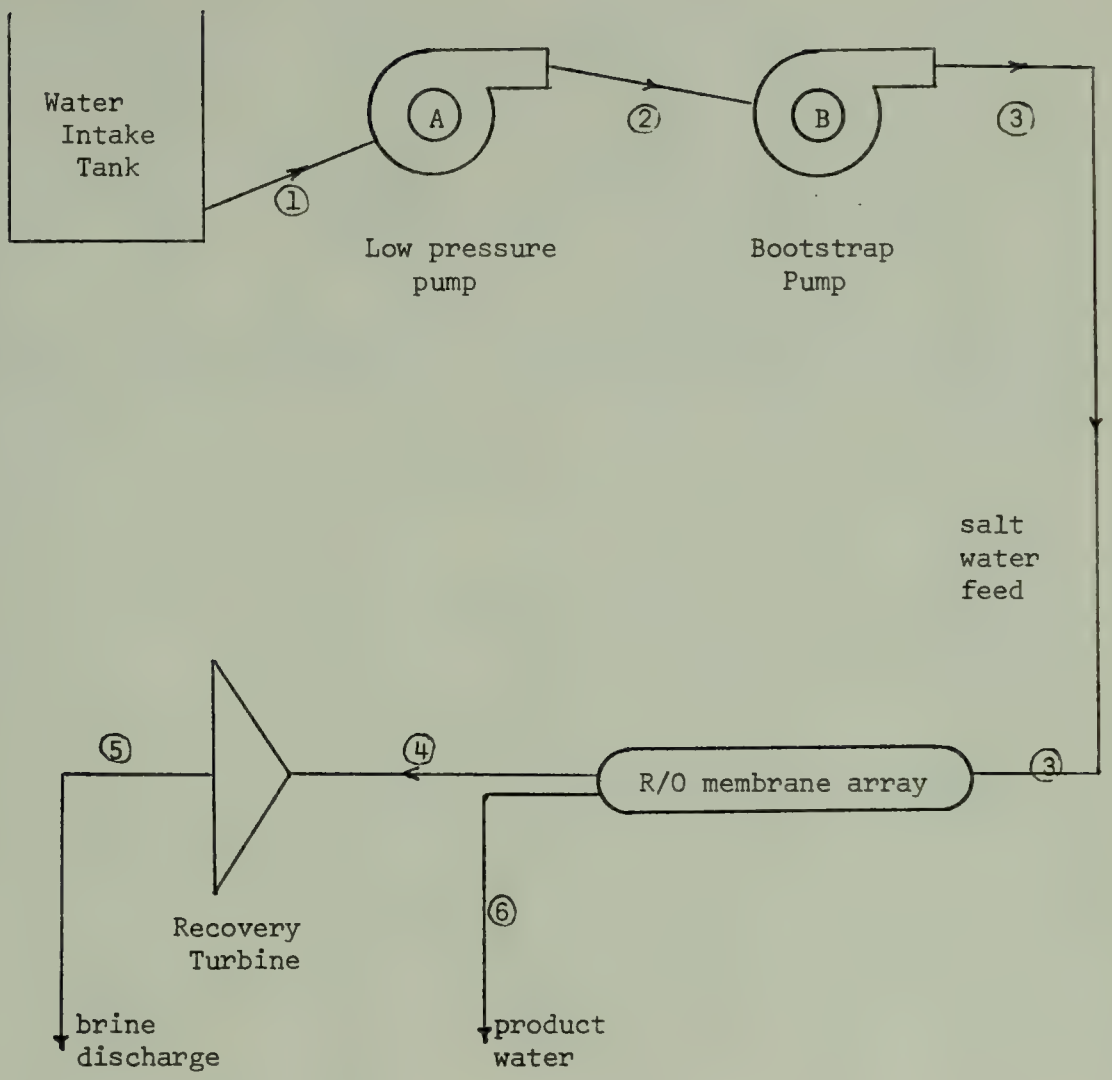

Figure (5): Simplified Process Flow Diagram

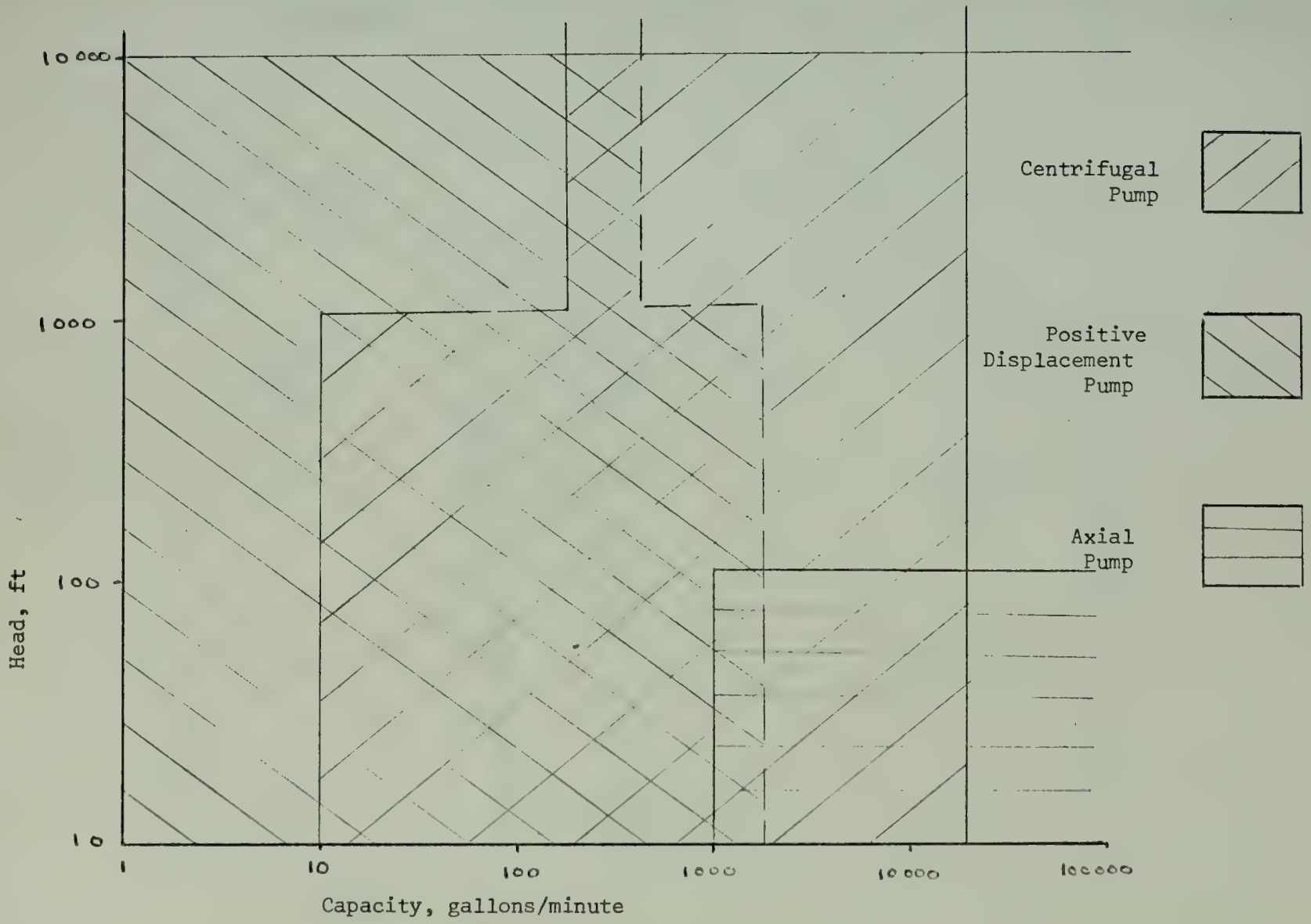

Figure (6): General domains of operation of standard pumping equipment

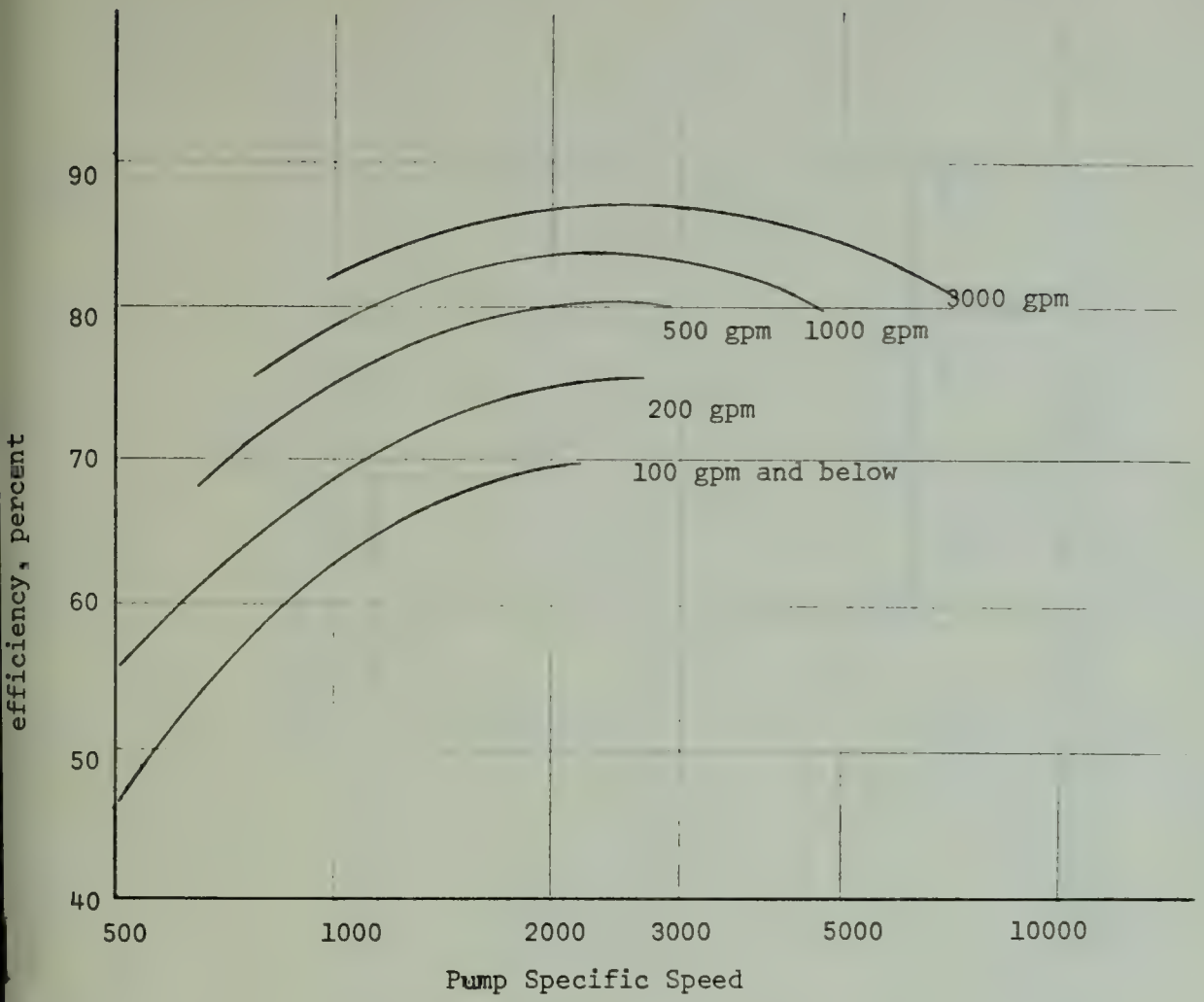

Figure (7): Single stage turbopump efficiencies (Worthington data)

Centrifugal Mixed-Flow Propeller

Form of dynamic pump impellers related to specific speed

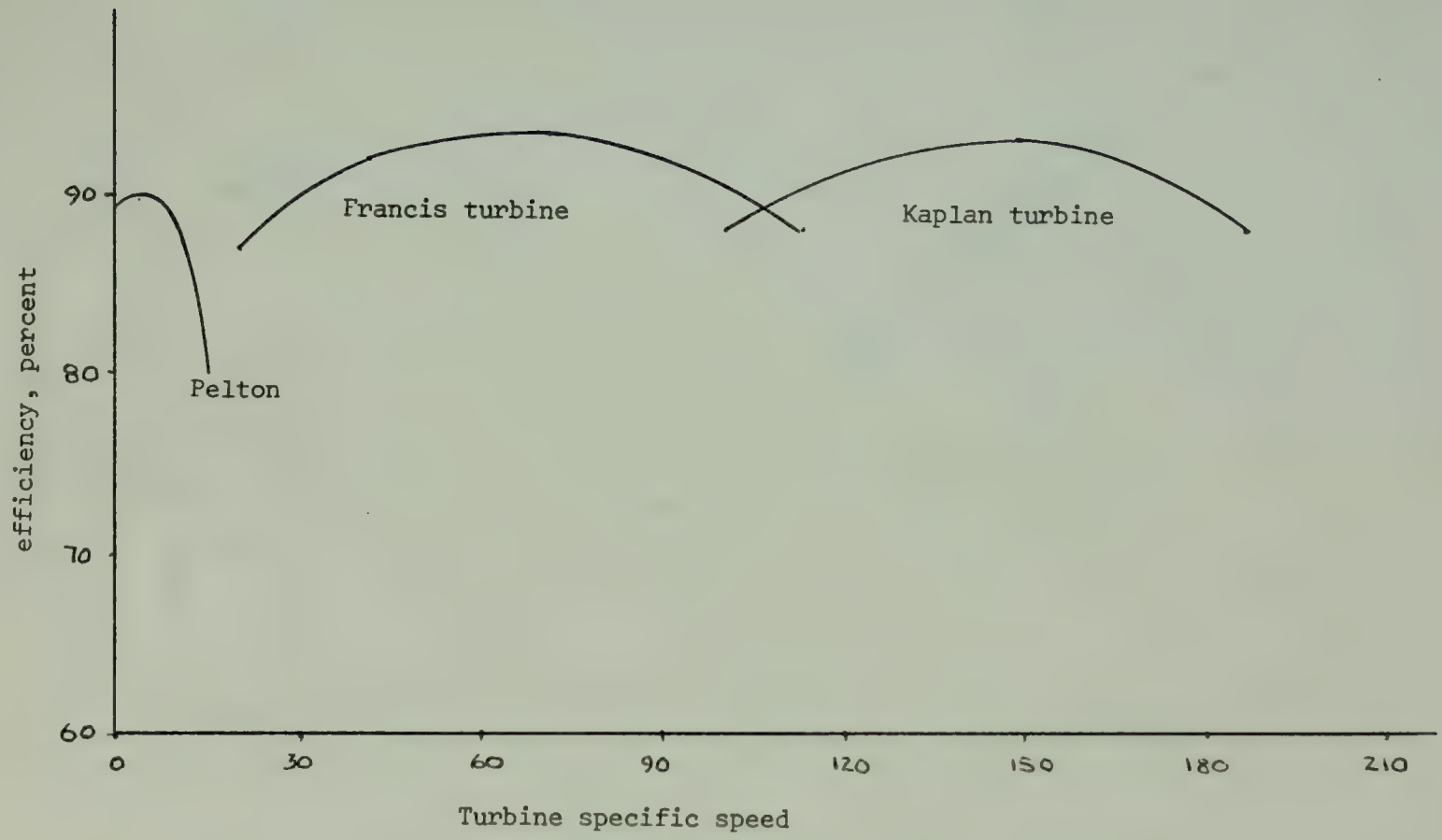

Figure (8): Single stage hydraulic turbine efficiencies

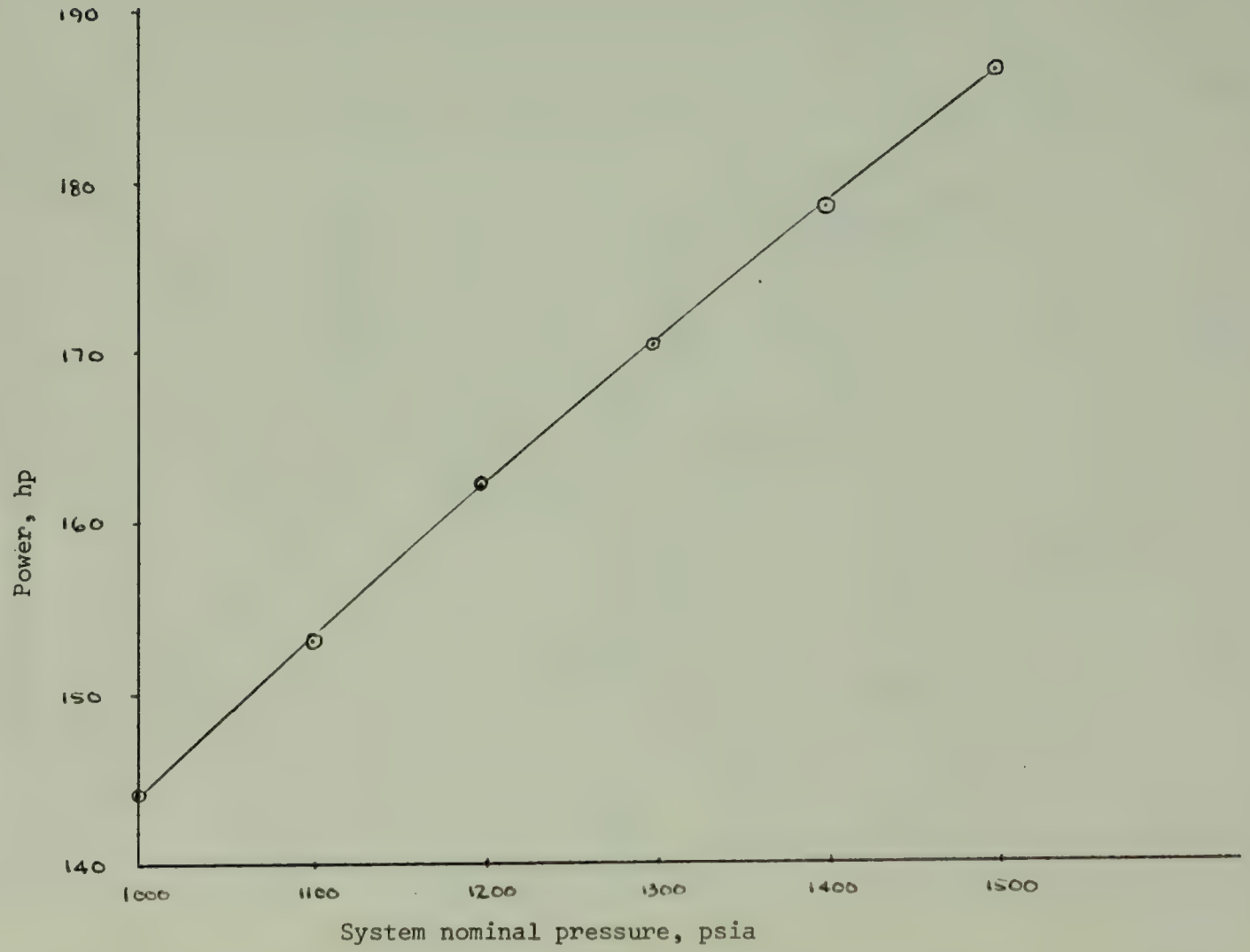

Figure (9): Low pressure pump power as a function of system nominal pressure

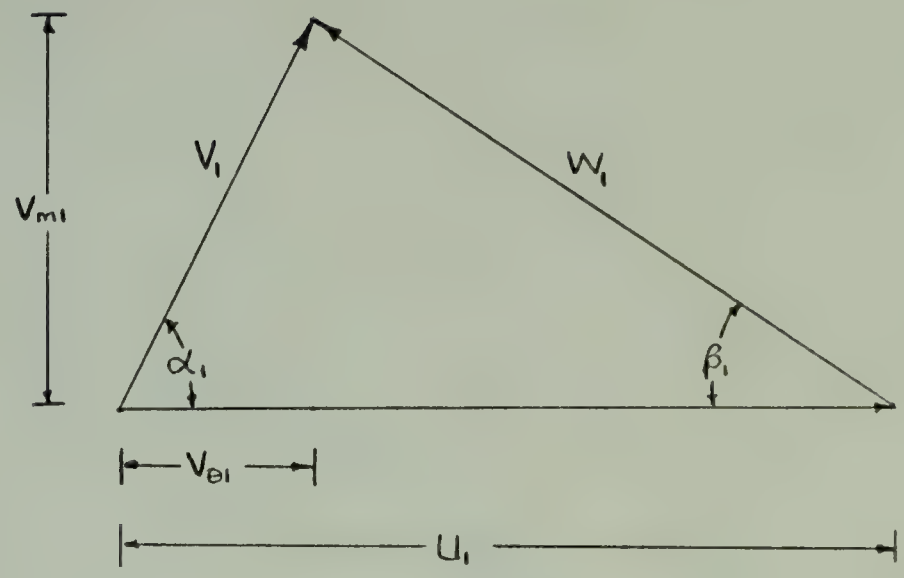

a) Entrance

b) Discharge

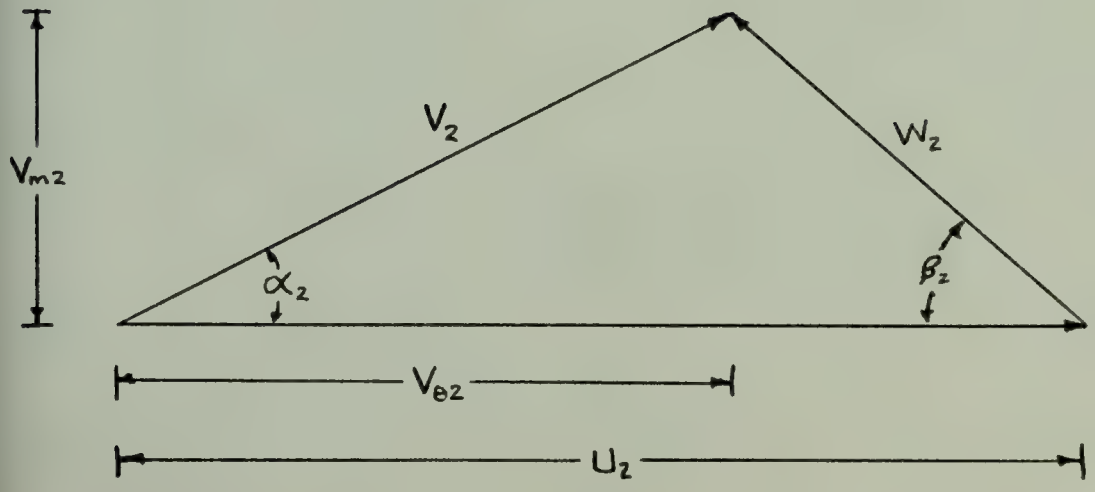

Figure (10): Entrance and discharge velocity triangles for a centrifugal pump

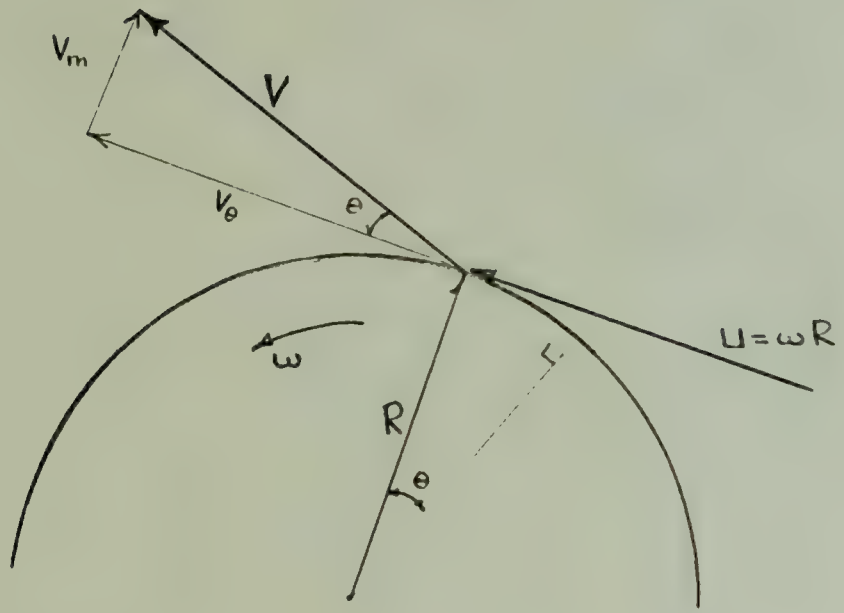

Figure (11): Velocity components at discharge from a radial turbine

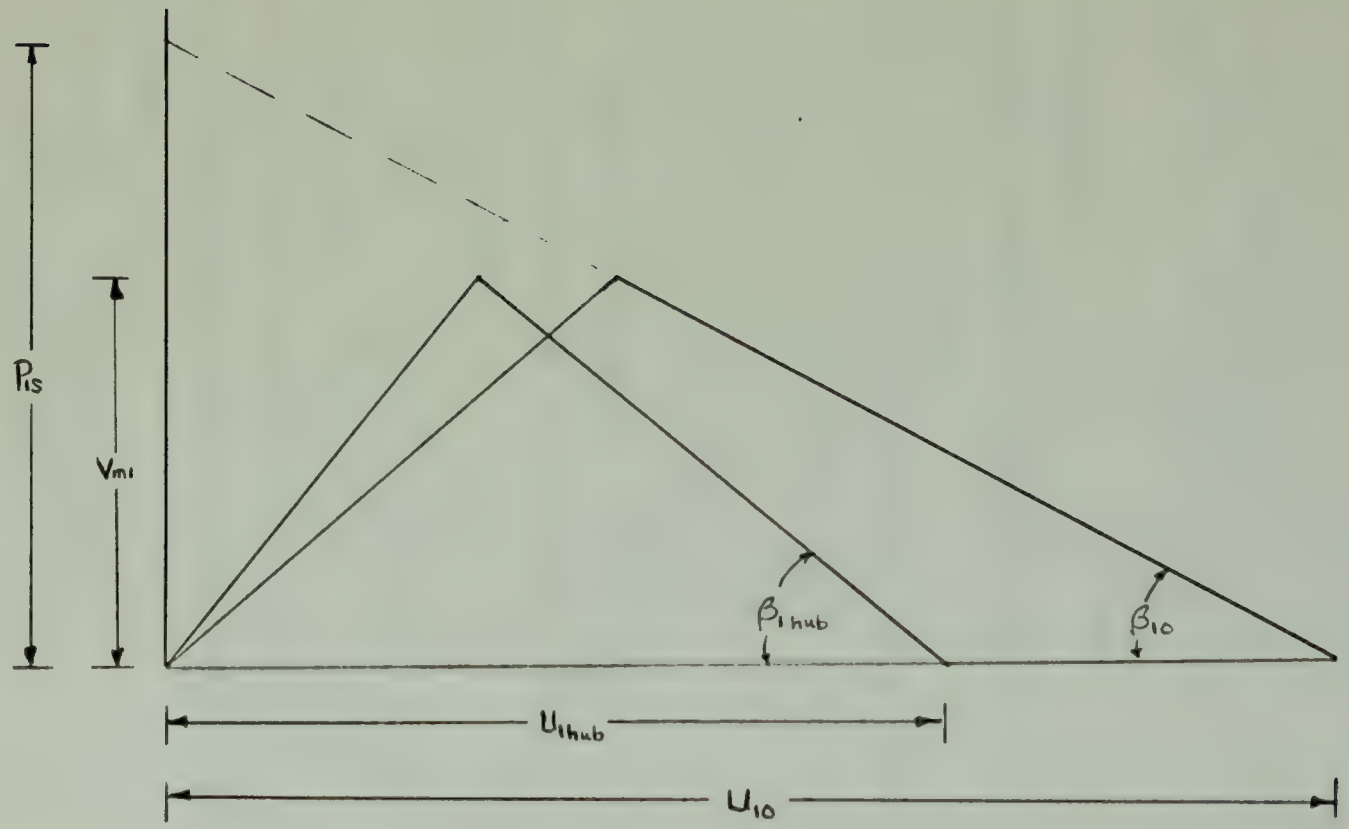

Figure (12): Inlet velocity diagram (hub and outer edge)

APPENDIX A

PROCESS AND CALCULATIONS TO YIELD MINIMUM INTAKE PUMP POWER

This appendix outlines the process used to determine that pump/recovery turbine combination which requires the minimum amount of external power input to the reverse osmosis system. Results of calculations are provided.

1. Turbine characteristics

a) As discussed in Chapter III, a Francis turbine with a specific speed of $N_{s,t} = 20$ is initially chosen.

b) Turbine inlet pressure is assumed to equal the system nominal pressure minus 10 percent of the system nominal pressure (to account for losses across the membrane). The head across the turbine is denoted by H_t^*. It is assumed that the back pressure is 25 psia.

$$H_t^* = (\text{Turbine inlet pressure} - 25 \text{ psia}) \frac{33.93}{14.7}, \text{ ft}$$

The limiting head per stage is 800 ft, as suggested by Carmichael [7]. The number of stages is denoted by n_t.

$$n_t = H_t^*/800, \text{ or next higher integer if non-integral}$$

The head across a turbine stage is denoted by H_t; $H_t = H_t^*/n_t$.

With the brine flow rate taken from the table on figure (4), and the definition of turbine specific speed, the turbine rotative speed can be determined.

$$N_{s,t} = \frac{N\, p^{1/2}}{H^{5/4}} = \frac{N[e_t \gamma Q_b H_t/550]^{1/2}}{H_t^{5/4}}$$

$$N_{s,t} = \frac{N[e_t \gamma Q_b/550]^{1/2}}{H_t^{3/4}} = 20$$

The turbine efficiency from figure (8), corrected for Reynolds number effects of sizing, yields an assumed e_t value of 0.80. And with a specific weight of sea water $\gamma = 64.0$ lbf/ft^3,

$$N = \frac{N_{s,t} H_t^{3/4}}{(0.305) Q_b^{1/2}} = 65.56 \frac{H_t^{3/4}}{Q_b^{1/2}}, \text{ rpm}$$

Since the recovery turbine and the bootstrap pump are on the same shaft, the turbine rotative speed is equal to the pump rotative speed.

d) Baumeister and Marks [3] indicate that the approximate number of Francis turbine buckets, Z, may be determined from the following empirical equation:

$$Z = 55/(N_{s,t})^{1/3}$$

For a turbine specific speed of 20, Z is 20.

And following an approach suggested by Carmichael, and presented in Jenkins [12], the loading factor can be utilized to determine the turbine rotor tip speed.

$$\xi = 1 - \frac{2}{Z} = 1 - \frac{2}{20} = 0.9$$

$$\xi = \frac{H_t g_o}{U_1^2} = 0.9$$

$$U_1^2 = H_t \frac{(32.2 \text{ ft/sec}^2)}{0.9}$$

$$U_1 = 5.98(H_t)^{1/2}, \text{ ft/sec}$$

And, since the turbine rotor diameter can be related to the rotor tip speed,

$$60 U_1 = \pi N D_r$$

the turbine rotor diameter can be found from

$$D_r = 19.10 \frac{U_1}{N}$$

2. Turbine Output Power and Bootstrap Pump Power and Head

a) From the definition of efficiency (neglecting mechanical loss)

$$P_t = \frac{\gamma Q_b H_t^*}{550} e_t$$

$$= 0.09309 \, Q_b H_t^*, \text{ hp}$$

when the turbine efficiency is 80 percent, as given above.

b) The power transferred from the bootstrap pump to the salt water feed is equal to the product of the turbine output power and the bootstrap pump efficiency.

$$P_p = P_t \eta_p = \frac{\gamma Q_p H_p^*}{550}$$

where P_p is pump output power, hp

Q_p is pump salt water flow rate, ft^3/sec

Hp^* is the total head developed across the pump, ft

η_p is the pump efficiency

From figure (7) a pump efficiency of approximately 77 percent is available for the flow rates under consideration in the specific speed region near $N_{s,p} = 3000$; with five percent deducted from this efficiency for Reynolds number sizing effects, a pump efficiency of 72 percent is obtained. And when the specific weight of salt water is included, the total head developed across the pump can be determined.

$$H_p^* = \frac{(0.72)550}{64} \frac{P_t}{Q_p} = 6.1875 \frac{P_t}{Q_p}, \text{ ft}$$

Since the limiting head per pump stage is 400 ft, denoting the number of pump stages by n_p,

$$n_p = \frac{H_p^*}{400}, \text{ or next higher integer if non-integral}$$

the head developed across a pump stage, H_p, can be determined

$$H_p = \frac{H_p^*}{n_p}$$

3. Bootstrap Pump Characteristics

a) As shown above, the head developed across a pump stage is a direct function of the turbine power and the salt water flow rate through the pump. Since the bootstrap pump is directly coupled to the energy recovery turbine, and the turbine rotative speed N has already been determined as above, the pump specific speed can be found.

$$N_s = \frac{N(Q_p)^{1/2}}{(H_p)^{3/4}}$$

b) Figure (10), taken from Percival [16], schematically shows the entrance and discharge velocity triangles for a pump. In a Lockheed Waterjet Propulsion System Study Report [24] wherein pump design is presented, it is suggested that the angle β_2 (shown in figure (10) be set at 22.5 degrees for preliminary estimation purposes, since this value produces highly efficient pumps with little dependence on other complicating factors. With the specific speed and an assumed value of β_2 = 22.5 degrees, the pump design chart of Stepanoff (figure 9.13 in [21]) is entered to find the head coefficient ψ.

c) The head coefficient is defined as the ratio of the pump head per stage to the square of the blade speed at the impeller exit U_2; the head coefficient is made dimensionless by inclusion of the acceleration due to gravity, g:

$$\psi = \frac{g\,H_p}{\pi^2 N^2 D_2^{\,2}} = \frac{g\,H_p}{U_2^{\,2}} \quad ,$$

The head coefficient is an extremely useful design parameter in that it relates the head to a maximum head theoretically available at zero flow capacity (with no flow prerotation). Using the above definition of head coefficient, the impeller diameter and blade tip speed can be found:

$$D_2 = \frac{60}{\pi N}\left(\frac{g\,H_p}{\psi}\right)^{1/2} = 108.375\,\frac{1}{N}\left(\frac{H_p}{\psi}\right)^{1/2}$$

and

$$U_2 = \frac{\pi N}{60}\,D_2 = \frac{1}{19.10}\,N\,D_2$$

where N is rotative speed in rpm
D_2 is impeller diameter in feet

4. Low Pressure Pump Power

a) The difference between the system nominal head and the actual head developed across the bootstrap pump is the remaining head H_R^*: that is

$$H_R^* = H_n^* - H_p^*$$

The flow rate of feed water through the low pressure pump is equal to the flow rate of feed water through the bootstrap pump; therefore a dynamically similar pump with the same efficiency is assumed. Then the power which must be input to the low pressure pump is the product of the remaining head and the feed water flow rate, divided by the low pressure pump efficiency:

$$P_{lp} = \frac{H_R^* \gamma Q_p}{(0.72)550} = 0.1616\,H_R^*\,Q_p,\ hp$$

Table 2 : Results of Calculations for Appendix A

System Nominal Pressure, psia	1000	1100	1200	1300	1400	1500
Turbine Inlet Pressure, psia	900	990	1080	1170	1260	1350
H_t*, ft	2019.5	2227	2329	2643	2850	3058
Number of turbine stages	3	3	3	4	4	4
H_t, ft	673.2	742.4	776.5	660.7	712.6	764.5
Rotative speed N, rpm	12723	14064	14905	13578	14679	15864
Rotor tip speed U_1, ft/sec	155	163	167	154	160	165
Rotor diameter D_1, ft	0.2329	0.2213	0.2135	0.216	0.2077	0.199
Turbine output power, hp	87.23	91.23	94.75	97.92	100.56	102.78
H_p*, ft	872	949	1023	1096	1165	1232
Number of bootstrap pump stages	3	3	3	3	3	3
Hp, ft	290.65	316.2	341	365.2	388.3	408
$N_{s,p}$	3012	3066	3012	2559	2597	2658
Angle β_2, degrees	22.5	22.5	22.5	22.5	22.5	22.5
Head coefficient,	0.43	0.43	0.43	0.45	0.445	0.44
Impeller diameter, ft	0.221	0.209	0.2048	0.2274	0.2181	0.208
Impeller tip speed, ft/sec	147	154	160	162	168	173
Remaining head, ft	1436	1591	1747	1904	2066	2230
L.P. pump power, hp	144	153	162	170	178	186

note: excessive rotative speed and 1.02 (max pump head per stage) for 1500 case; inclusion of additional stages would further degrade efficiency, increasing L.P. pump power for this case.

APPENDIX B
PROCESS AND CALCULATIONS FOR RECOVERY TURBINE DESIGN

This appendix outlines the process used to accomplish an initial design of the recovery turbine. Results of calculations are provided.

1. Input parameters for the turbine design

a) The mass flow rate of brine, $\dot{m}_b$ = 208.3 gallons per minute = 0.464 cubic feet per second

b) The turbine head per stage, H_t = 673.2 ft

c) The turbine specific speed, $N_{s,t}$ = 20

d) The loading factor, ξ = 0.9

e) The number of rotor blades, Z = 20

2. Rotor inlet calculations (subscript 3)

a) As used in Appendix A, the loading factor, ξ, is the ratio of the tangential component of the absolute entering velocity, $V_{\theta 3}$, and the rotor tip speed, U_3.

$$\xi = \frac{V_{\theta 3}}{U_3} = 0.9 \qquad \text{(B.1)}$$

If no swirl is allowed in the rotor discharge velocity, i.e. $V_{\theta 4} = 0$, then the loading factor can be used in Euler's equation:

$$P = -\frac{\dot{m}}{g_c}(U_4 V_{\theta 4} - U_3 V_{\theta 3})$$

$$V_{\theta 4} = 0$$

$$\therefore P = \frac{\dot{m}}{g_c} U_3 V_{\theta 3} = \frac{\dot{m}}{g_c} U_3^2 \xi \qquad \text{(B.2)}$$

From the calculations in Appendix A, the rotor tip speed, U_3 = 155 ft/sec. Then the power, using equation (B.2), is 36.5 hp developed per stage.

Therefore, the power developed across three identical stages is 109.5hp, which exceeds the value of 87.23 hp determined in Appendix A (with an assumed turbine overall efficiency of 80 percent). Since the same turbine and pump efficiencies were utilized for the six pressures evaluated, the overall conclusion of Appendix A will remain: the system nominal pressure of 1000 psia will still require the minimum amount of external power supply; however, the amount of external power required will be less than that value determined in Appendix A. Since the efficiency of the present design is greater than that value utilized in Appendix A, the rotative speed will be changed:

$$N_{s,t} = \frac{N\, P^{1/2}}{H^{5/4}}$$

yielding a new value N = 11351. Since the rotor tip speed, U_3, is related to the turbine stage head and loading factor, the tip speed is unchanged. However, the rotor tip diameter increases slightly from the first estimate:

$$D_3 = 19.10\, \frac{U_3}{N} = 0.26 \text{ ft} = 3.13 \text{ in}$$

b) From an approximate potential flow analysis, Carmichael [7] has established the following condition for avoiding negative velocities at the rotor inlet:

$$V_{m3} \geq \frac{2\pi}{Z} U_3 \qquad \text{(B.3)}$$

where V_{m3} is the meridional component of absolute velocity at rotor inlet, and
Z is the number of rotor blades

Therefore, the minimum value of V_{m3} is 48.7 ft/sec.

c) From geometry considerations,

$$\tan(\alpha_3) = \frac{V_{\theta 3}}{V_{m3}}$$

Since both $V_{\theta 3}$ and V_{m3} are related to U_3, equations (B.1) and (B.3) can be combined to yield the following equation for angle α_3:

$$(\alpha_3) = \tan^{-1}\left(\frac{Z-2}{2\pi}\right)$$

And for 20 rotor blades, $\alpha_3 = 70.75°$

d) With U_3, $V_{\theta 3}$, α_3, and a minimum value of V_{m3} known, the remaining components of the rotor inlet velocity triangle can be determined:

$$V_3 = V_{m3} \sec(\alpha_3) = 147.7 \text{ ft/sec}$$

$$\beta_3 = \tan^{-1}\left(\frac{V_{\theta 3} - U_3}{V_{m3}}\right) = \tan^{-1}\left(\frac{-0.1\ U_3}{V_{m3}}\right) = -17.6°$$

$$W_3 = V_{m3} \sec(\beta_3) = 51.1 \text{ ft/sec}$$

e) With the rotor diameter determined, the blade height t can be obtained by using the continuity equation for incompressible flow:

$$Q_b = \pi D_3 t_3 V_{m3}$$

which yields a value $t_3 = 0.0117$ ft

3. Rotor outlet calculations (subscript 4)

a) A major assumption in the previous section was that the tangential component of the discharge velocity was zero; with this simplification, then, the loading factor could be readily used in Euler's power equation (B.2) Therefore, $V_{\theta 4} = 0$.

b) Carmichael [7] suggests that angle β_4 take on a value of -60°, and this value will be assumed here.

c) In order to proceed in the analysis, a diameter ratio is necessary. Then, assuming a mean diameter ratio of 0.4 at the mean inner diameter, $d_4 = 1.252$ in, at a first cut.

d) With this assumed mean diameter d_4, a blade speed is determined:

$$\text{mean } U_4 = \frac{N D_4}{19.10} = 62 \text{ ft/sec}$$

e) With U_4, β_4, and a right angle as known quantities, the remaining components of the mean outlet velocity diagram can be determined:

$$V_4 = U_4 \cot(\beta_4) \text{ at mean outlet}$$

$$W_4 = U_4 \csc(\beta_4) \text{ at mean outlet}$$

Then $V_4 = 35.8$ ft/sec and $W_4 = 71.6$ ft/sec at mean outlet.

f) The continuity equation for incompressible flow can be utilized to find the annular flow area, and then the blade height can be determined, using V_4 since $V_{\theta 4} = 0$.

$$A_{\text{annular}_4} = \frac{Q}{V_4} = 0.01296 \text{ ft}^2$$

$$t_4 = \frac{A_{\text{annular}, 4}}{2\pi r_{4\text{mean}}} = 0.0395 \text{ ft}$$

One-half of the blade height, when subtracted from the assumed outlet mean radius, yields the outlet radius at the hub:

$$r_4 - \frac{t_4}{2} = 0.389 \text{ in}$$

which appears to leave enough space in which to fit a shaft. Therefore, the initial assumption of the mean outlet diameter at a value of 0.4 the inlet diameter will not be changed.

4. Stator calculations

a) If it is assumed that the gap between the stator outlet and the rotor inlet is small,and that the moment of momentum is constant across the gap, then the velocity triangle at stator outlet is effectively the same as that of the rotor inlet; therefore, further calculation is not necessary.

b) If it is assumed that the number of stator blades equals the number of rotor blades, then the radial spacing between blades, s, can be found (subscript 2 - stator outlet; subscript 1 - stator inlet):

$$s = \frac{\pi D_2}{Z} = 0.492 \text{ in}$$

With an assumed pitch (the radial spacing between blades) - chord ratio of 0.6, and following the development presented in Potter [17], the approximate value of the radius at stator inlet is determined:

$$R_1 = \left\{ \left[R_2 + C \cos \left(\frac{\pi}{Z} + \alpha_3 \right) \right]^2 + \left[C \sin \left(\frac{\pi}{Z} + \alpha_3 \right) \right]^2 \right\}^{1/2}$$

$$R_1 = 1.892 \text{ in}, \quad D_1 = 3.784 \text{ in}$$

APPENDIX C
PROCESS AND CALCULATIONS FOR BOOTSTRAP PUMP DESIGN

This appendix outlines the process used to accomplish an initial design of the bootstrap pump. Results of calculations are provided.

1. Input parameters for the bootstrap pump design

a) The mass flow rate of salt water, $\dot{m}_{sw}$ = 277.8 gallons per minute = 0.619 cubic feet per second.

b) The rotative speed of the pump, N = 11351 rpm.

2. Determination of pump head developed per stage, and specific speed

a) In Appendix B, the actual power developed across each of three recovery turbine rotors was calculated to be 36.5 hp; therefore, the total power across three identical stages is 109.5 hp. If it is assumed that, due to the losses in distribution from one stage to the next, and the mechanical losses, 4.5 hp is lost, then the total power available as input to the bootstrap pump is 105 hp. Then, following the procedure developed in Appendix A, the total head across the pump can be determined.

$$Hp^* = \frac{(0.72)550}{64} \frac{Pt}{Q_p} = 6.1875 \frac{(105)}{0.619} = 1049 \text{ ft}$$

Keeping the limiting head per stage to 400 ft, the number of pump stages can be determined

$$n_p = \frac{Hp^*}{400}, \text{ or next higher integer if non-integral}$$

$$n_p = 3$$

and then the head developed across a pump stage is set

$$Hp = 344.7 \text{ ft}$$

b) The specific speed of the bootstrap pump is then determined

$$N_{s,p} = N \frac{(Q_p)^{1/2}}{(Hp)^{3/4}} = 2340$$

Reference to figure (7), which relates pump efficiency to specific speed and flow rates, shows that the curve is relatively flat in this region, so the assumed pump efficiency of 0.72 appears to be a satisfactory estimate.

3. Impeller discharge conditions

a) As stated in Stepanoff [21] and in the Lockheed Waterjet Propulsion report [24], the vane discharge angle is the most important single design element: theoretical characteristics are determined by this angle; and in practice, the vane discharge angle remains the deciding factor. As recommended in both the Lockheed report and in Stepanoff, an average value of β_2 is 22 1/2°; this value will be utilized in this thesis.

b) A speed constant relating the impeller peripheral velocity at a free jet velocity under a head Hp can be defined as follows:

$$K_u = \frac{U_2}{(2_g Hp)^{1/2}}$$

Since the pump head is known, the impeller peripheral velocity can be determined; and, knowing the rotative speed, the impeller diameter can be determined. At a specific speed of 2340, the speed constant value from Stepanoff [figure 5.2 in 21] is $K_u = 1.06$ (when based on a mean discharge diameter D_{2m} defined below) and $K_u = 1.10$ (when based on the impeller discharge outer diameter D_{20}).

$$U_{2m} = 1.06\ (2_g Hp)^{1/2} = 159 \text{ ft/sec}$$

$$U_{20} = 1.10\ (2_g Hp)^{1/2} = 165.1 \text{ ft/sec}$$

Since the impeller diameter is related to the peripheral velocity by the rotative speed, the impeller mean discharge diameter, D_{2m}, and the impeller

discharge outer diameter are readily obtained.

$$D_{2m} = \frac{60}{\pi N} U_{2m} = 0.2675 \text{ ft}$$

$$D_{20} = \frac{60}{\pi N} U_{20} = 0.2778 \text{ ft}$$

And from Stepanoff's definition of the mean discharge diameter, the impeller discharge inner diameter is found.

$$D_{2m} = \left[\frac{D_{20}^2 + D_{2i}^2}{2} \right]^{1/2}$$

$$D_{2i} = \left[2 D_{2m}^2 - D_{20}^2 \right]^{1/2} = 0.2568 \text{ ft}$$

c) The above development was based on a speed constant derived from conventional designs in which the number of impeller vanes is correlated to the impeller discharge angle (in degrees) by the following "rule of thumb":

$$Z = \frac{\beta_2}{3}$$

which yields 8 impeller vanes. Therefore, a value of 8 will be used for the number of impeller vanes.

d) The frequently used capacity coefficient, ϕ, is the ratio of the meridional component of the impeller absolute discharge velocity to the impeller discharge peripheral velocity:

$$\phi = \frac{V_{m2}}{U_2}$$

The capacity coefficient is a function of both the impeller discharge angle, β_2, and the specific speed, $N_{s,p}$; from figure 9.15 in Stepanoff [1], the appropriate value of ϕ is 0.17. With this value, the meridional

component of the impeller discharge velocity is readily determined, when based on the mean impeller discharge blade speed.

$$V_{m2} = \phi\ U_{2m} = 27 \text{ ft/sec}$$

e) With the impeller discharge angle assumed to be 22.5° and the values for blade peripheral speed and V_{m2} determined as above, the remainder of the discharge triangle can be determined.

$$W_2 = V_{m2} \csc(\beta_2) = 70.55 \text{ ft/sec}$$

$$W_{\theta 2} = W_2 \cos(\beta_2) = 65.2 \text{ ft/sec}$$

$$V_{\theta 2} = U_2 - W_{\theta 2} = 93.8 \text{ ft/sec}$$

$$\alpha_2 = \tan^{-1} \csc(\alpha_2) = 98 \text{ ft/sec}$$

4. Impeller entrance conditions

a) Stepanoff [21] indicates that a normal ratio of impeller entrance velocity (meridional component) to impeller discharge velocity (meridional component) is 1.5, and that for multistage pumps the ratio V_{m1}/V_{m2} may be as high as 1.625. For this thesis a ratio 1.5 will be assumed; then V_{m1} = 40.5 ft/sec. Additionally, Stepanoff provides a ratio of the diameter of the outer edge of the impeller entrance (D_{1O}) to the mean discharge diameter (D_{2m}), which at the appropriate specific speed is 0.6. The continuity equation for incompressible flow can be utilized to determine the inner diameter at the impeller entrance (D_{1i}), assuming that the flow is normal to the dimension ($D_{1O} - D_{1i}$).

$$V_{m1} \frac{\pi}{4} (D_{1O}^2 - D_{1i}^2) = Q_p$$

Substitution of the appropriate values yields D_{1i} = 0.0794 ft = 0.953 in.

b) Since the rotative speed is known, and the outer edge of the impeller entrance diameter is known, the peripheral velocity at the

outer edge of the impeller entrance can be determined. If a mean impeller entrance diameter be defined in a way analogous to that for the exit, i.e., $D_{1m} = \left[\frac{D_{10}^2 + D_{1i}^2}{2}\right]^{1/2}$, then the velocity triangle at the mean impeller entrance diameter can be determined. Then, with $D_{1m} = 0.01603$ft and a rotative speed of 11351 rpm, the blade speed at impeller mean entrance diameter is $U_{1m} = 9.53$ ft/sec. At the outer edge of the impeller entrance the peripheral velocity is $U_{10} = 95.4$ ft/sec. Due to the marked change in impeller blade speed with impeller entrance diameter, a set of entrance velocity trangles would be necessary. However, the values for only the entrance outer edge are provided here. Referring to figure (12), since V_{m1} and U_1 are known at various points at the impeller entrance, the remainder of the velocity triangle can be determined, utilizing another rule of thumb from Stepanoff [21]. With some "nominal" pre-rotation of the flow allowed, the ratio of pitch per second to inlet meridional velocity, P_{1s}/V_{m1} varies within narrow limits (1.15 to 1.25)--see figure (12) for further definition -- and a value of 1.2 will be utilized herein. Then, at the outer edge of the impeller entrance,

$$\beta_{10} = \tan^{-1}\left(\frac{P_{1s}}{U_{10}}\right) = \tan^{-1}\left(\frac{1.2\ V_{m1}}{U_{10}}\right) = 27°$$

$$W_{\theta 1} = V_{m1} \cot(\beta_{10}) = 79.5 \text{ ft/sec}$$

$$V_{\theta 1} = U_{10} - W_{\theta 1} = 15.9 \text{ ft/sec}$$

$$V_1 = (V_{\theta 1}^2 + V_{m1}^2)^{1/2} = 43.5 \text{ ft/sec}$$

$$W_1 = V_{m1} \csc(\beta_{10}) = 89.2 \text{ ft/sec}$$

5. Impeller discharge blade height

a) If the impeller discharge mean diameter is considered the

representative exit diameter dimension, then the blade height, can be determined by using the continuity equation for incompressible flow.

$$Q_p = \pi D_{2m} t \, V_{m2}$$

Substitution of the appropriate values for the volumetric flow rate, the mean discharge diameter, and the absolute velocity (meridional component) yields the value of t = 0.0273 ft.

APPENDIX D
PROCESS AND CALCULATIONS FOR LOW PRESSURE PUMP DESIGN

This appendix outlines the process used to accomplish an initial design of the low pressure pump. Results of calculations for the system nominal pressure under consideration, P_s = 1000 psia, are presented.

1. Input parameters for low pressure pump design

a) The mass flow rate of salt water, $\dot{m}_{sw}$ = 277.8 gallons per minute = 0.619 cubic feet per second.

b) The specific speed of the low pressure pump is equal to that of the bootstrap pump; $N_{s,lp}$ = 2340

2. Determination of NPSH and rotative speed, N

a) The definition of NPSH was presented in Chapter IV.

$$NPSH = H + \frac{V_{ml}^2}{2g} - H_{vapor}$$

If it is assumed that the pump suction is effectively from a tank with a salt water depth of 10 feet, under atmospheric pressure; if a meridional velocity V_{ml} is taken as the same as that value determined for the bootstrap pump; and if the vapor pressure for the salt water feed can be assumed to be equal to that of fresh water at 90°F, then NPSH can be determined:

NPSH = 10 ft + 33.93 ft + 25.46 ft - 1.61 ft = 67.78 ft

b) From the definition of suction specific speed presented in Chapter IV, the pump upper rotative speed limit can be determined.

$$S = \frac{N\, Q^{1/2}}{(NPSH)^{3/4}} \leq 8000$$

With S = 8000,

$$N = S(NPSH)^{3/4}/Q^{1/2} = 11339 \text{ rpm}$$

That is, in order to avoid cavitation in the low pressure pump, the rotative speed of that pump should be less than or equal to 11339 rpm.

3. Determination of pump head developed per stage

a) In order to have the low pressure pump operate with characteristics similar to those of the bootstrap pump, the specific speeds of the two pumps should be the same; as stated above, $N_{s,lp} = 2340$. The definitions of specific speed and of suction specific speed, both applied to the low pressure pump result in determination of the maximum limit for the head developed per low pressure pump stage.

$$\frac{N_{s,lp}}{S_{lp}} = \frac{N \dfrac{(Q_{lp})^{1/2}}{(H_{lp})^{3/4}}}{N \dfrac{(Q_{lp})^{1/2}}{(NPSH)^{3/4}}} = \frac{(NPSH)^{3/4}}{(H_{lp})^{3/4}}$$

$$H_{lp} = (NPSH)\left(\frac{S_{lp}}{N_{s,lp}}\right)^{4/3} = 349 \text{ ft}$$

That is, in order to avoid cavitation in the low pressure pump, the head developed per stage across the low pressure pump should be less than or equal to 349 ft.

b) As presented in Appendix A, the difference between the system nominal head and the actual head developed across the bootstrap pump is termed the remaining head, H_R*;

$$H_R^* = H_n^* - Hp^* = (2308 - 1049)\text{ft} = 1259 \text{ ft}$$

c) From the limiting head per stage as determined in part 3(a) above, the number of low pressure pump stages is determined:

$$n_{lp} = \frac{H_R^*}{349 \text{ ft}} = 3.6 \rightarrow 4 \text{ stages}$$

Then $H_{lp} = 314.75$ ft. And 314.75 ft is less than 349 ft.

d) Having determined the actual head developed per low pressure pump stage, the rotative speed constraint must be checked.

$$N = N_{s,lp} (H_{lp})^{3/4}/(Q_{lp})^{1/2} = 10491 \text{ rpm}$$

And 10491 is less than 11339 rpm, so the rotative speed constraint is satisfied.

It is now possible to commence the pump design along the lines presented in Appendix C for the bootstrap pump. The procedure to be followed is nearly identical to that presented in Appendix C; therefore, much of the explanatory narrative can be omitted in this appendix. The symbology used in the remainder of this appendix is the same as that of Appendix C.

4. Impeller discharge conditions

a) $\beta_2 = 22.5°$, assumed as in Appendix C

b) The speed constant K_u leads to determination of impeller peripheral velocity and impeller diameter.

$$U_{2m} = 1.06 (2_g H_{lp})^{1/2} = 150.9 \text{ ft/sec}$$

$$U_{20} = 1.10 (2_g H_{lp})^{1/2} = 156.6 \text{ ft/sec}$$

$$D_{2m} = \frac{60}{\pi N} U_{2m} = 0.2747 \text{ ft}$$

$$D_{20} = \frac{60}{\pi N} U_{20} = 0.2851 \text{ ft}$$

$$D_{2i} = 0.2639 \text{ ft}$$

c) The number of impeller vanes is 8.

d) The capacity coefficient, as a function of the same specific speed and the same discharge angle as for the bootstrap pump, is unchanged; $\phi = 0.17$

$$V_{m2} = \phi U_{2m} = 25.65 \text{ ft/sec}$$

e) The remaining portions of the impeller discharge triangle are readily determined from geometrical and trigonometrical consideration.

$$W_2 = V_{m2} \csc(\beta_2) = 67 \text{ ft/sec}$$

$$W_{\theta 2} = W_2 \cos(\beta_2) = 61.9 \text{ ft/sec}$$

$$V_{\theta 2} = U_2 - W_{\theta 2} = 89 \text{ ft/sec}$$

$$\alpha_2 = \tan^{-1}\left(\frac{V_{m2}}{V_{\theta 2}}\right) = 16.1°$$

$$V_2 = V_{m2} \csc(\alpha_2) = 92.6 \text{ ft/sec}$$

5. Impeller entrance conditions

a) Assuming, as in Appendix C, that the ratio between inlet and outlet meridional components of the absolute velocities is 1.5, the value of V_{m1} is readily set at $V_{m1} = 38.48$ ft/sec. Applying the same assumptions as those stated in Appendix C, the inner diameter at the impeller entrance is determined. $D_{1i} = 0.08176$ ft = 1.06 in.

b) When mean entrance impeller diameter is defined in a way analogous to that for the exit, i.e.,

$$D_{1m} = \left[\frac{D_{10}^2 + D_{1i}^2}{2}\right]^{1/2}$$

the velocity triangle at this diameter can be determined. D_{1m} is calculated

to be 0.01693 ft. The blade speed (peripheral velocity) at this diameter is 9.3 ft/sec. At the outer edge of the impeller entrance the peripheral velocity is 90.5 ft/sec.

c) Using the equations presented in section 4(b) of Appendix C, and making the same assumptions as described therein, the remainder of the velocity triangle can be determined at the outer edge of the impeller entrance.

$$\beta_{10} = \tan^{-1}\left(\frac{1.2\ V_{m1}}{U_{10}}\right) = 27°$$

$$W_{\theta 1} = V_{m1} \cot(\beta_{10}) = 75.5 \text{ ft/sec}$$

$$V_{\theta 1} = U_{10} - W_{\theta 1} = 15 \text{ ft/sec}$$

$$V_1 = (V_{\theta 1}^2 + V_{m1}^2)^{1/2} = 41.3 \text{ ft/sec}$$

$$W_1 = V_{m1} \csc(\beta_{10}) = 84.76 \text{ ft/sec}$$

6. Impeller discharge blade height

a) If the impeller discharge mean diameter is considered the representative exit diameter dimension, then the blade height, t, can be determined by using the continuity equation for incompressible flow, as was accomplished in Appendix C.

$$Q_p = \pi D_{2m} t V_{m2}$$

Substitution of the appropriate values yields the value of t = 0.0273 ft.

7. Determination of low pressure pump power

a) The product of the remaining head and the salt water flow rate, divided by the pump efficiency, is the power which must be input to the low pressure pump:

$$P_{lp} = \frac{H_R^* \gamma Q_p}{(0.72)550} = 125.94 \text{ hp}$$

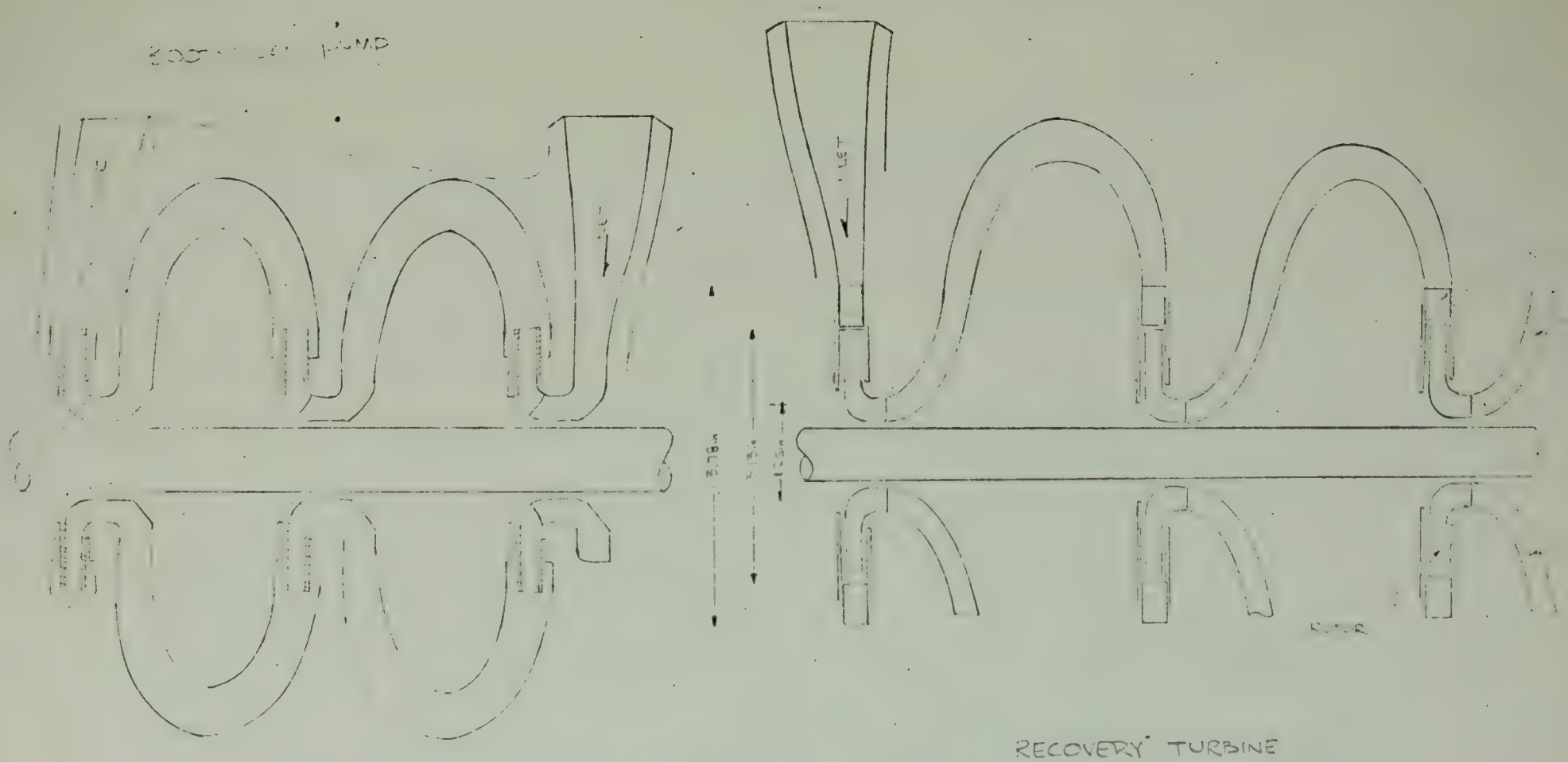

RECOVERY TURBINE

Thesis
A7148 Armstrong 153111
Energy recovery in the reverse osmosis process.